Bacillus subtilis RecA interacts with and loads RadA/Sms to unwind recombination intermediates during natural chromosomal transformation

Rubén Torres, Ester Serrano and Juan C. Alonso [ID]*

Department of Microbial Biotechnology, Centro Nacional de Biotecnología, CNB-CSIC, 28049 Madrid, Spain

ABSTRACT

During natural transformation *Bacillus subtilis* RecA, polymerized onto the incoming single-stranded (ss) DNA, catalyses DNA strand invasion resulting in a displacement loop (D-loop) intermediate. A null *radA* mutation impairs chromosomal transformation, and RadA/Sms unwinds forked DNA in the 5′→3′ direction. We show that in the absence of RadA/Sms competent cells require the RecG translocase for natural chromosomal transformation. RadA/Sms tetracysteine motif (C13A and C13R) variants, which fail to interact with RecA, are also deficient in plasmid transformation, but this defect is suppressed by inactivating *recA*. The RadA/Sms C13A and C13R variants bind ssDNA, and this interaction stimulates their ATPase activity. Wild-type (*wt*) RadA/Sms interacts with and inhibits the ATPase activity of RecA, but RadA/Sms C13A fails to do it. RadA/Sms and its variants, C13A and C13R, bound to the 5′-tail of a DNA substrate, unwind DNA in the 5′→3′ direction. RecA interacts with and loads *wt* RadA/Sms to promote unwinding of a non-cognate 3′-tailed or 5′-fork DNA substrate, but RadA/Sms C13A or C13R fail to do it. We propose that *wt* RadA/Sms interaction with RecA is crucial to recruit the former onto D-loop DNA, and both proteins in concert catalyse D-loop extension to favour integration of ssDNA during chromosomal transformation.

INTRODUCTION

Natural transformation contributes to the acquisition of genetic diversity and to the restoration of mutated genes, playing a central role in the evolution and the spread of metabolic pathways, pathogenicity traits and antibiotic resistance genes (1,2). Natural competence, which is a bacterium-programmed mechanism of horizontal gene transfer, is induced in response to different types of stress and activated through a dedicated host-encoded transcriptional programme (3–5). During *Bacillus subtilis* natural competence development, DNA replication is halted, a transcriptional program is activated and the membrane-specific DNA uptake apparatus is transiently assembled at one of the cell poles (3). The DNA uptake apparatus binds any extracellular double-stranded (ds) DNA, linearizes it, degrades one strand, and internalizes the other strand into the cytosol (3–5). The essential single-stranded binding protein, SsbA, and the competence-specific, SsbB, are proposed to coat and protect the incoming linear single-stranded (ss) DNA as soon as it leaves the entry channel (6–9).

In the ATP·Mg^{2+} bound form, RecA (RecA·ATP) from natural competent *B. subtilis* and *Streptococcus pneumoniae* cells can filament onto ssDNA, but this RecA nucleoprotein filament (or RecA-ssDNA complex) cannot catalyse DNA strand exchange *in vitro* (10–12). *B. subtilis* RecA cannot nucleate on the SsbA-ssDNA (or SsbA-ssDNA-SsbB) complexes (7,13). These inabilities are overcome with the help of the two-component mediators (SsbA in concert with DprA or RecO [in the Δ*dprA* context]). A two-component mediator promotes RecA·ATP nucleation and filament growth onto SsbA- (or SsbA and SsbB)-coated ssDNA with a subsequent activation to catalyse DNA strand exchange (8,9). Then, RecA·ATP polymerises on the ssDNA and undergoes cycles of polymerization/depolymerization to ensure formation of a nucleoprotein filament emanating from the entry channel towards the nucleoid (RecA threads) (8,9,14,15). A RecA·ATP nucleoprotein filament, with the help of a two-component mediator, efficiently searches for and identifies a homologous sequence. Once a region of homology is found, RecA·ATP promotes DNA strand invasion to produce a metastable (displacement loop [D-loop]) intermediate, leading to heteroduplex DNA. RecA·ATP, which is a slow motor (hydrolyses ∼9 ATP min^{-1}), might not be able to branch migrate over long stretches of DNA. Unless stated otherwise, the indicated genes and products are of *B. subtilis* origin.

Bacillus subtilis encodes three branch migration translocases, RuvAB, RecG and RadA/Sms (the slash between

---

*To whom correspondence should be addressed. Tel: +34 91585 4546; Fax: +34 91585 4506; Email: jcalonso@cnb.csic.es

RadA and Sms names denotes that they have alternative names, the gene is termed *radA*) (16–18). The absence of RuvAB or RecG has no negative impact in chromosomal and plasmid transformation (5), but a null *radA* mutant (Δ*radA*) reduces ∼140-fold chromosomal transformation, but not plasmid transformation in otherwise *wild type (wt)* cells (18). Similarly, *S. pneumoniae* RadA (henceforth referred to as RadA$_{Spn}$), which shares ∼62% sequence identity with RadA/Sms, is involved in natural chromosomal transformation, but Δ*radA$_{Spn}$* cells have a plasmid transformation rate close to the *wt* control (19,20). RadA might help RecA to extend the D-loop intermediates (18,20). Alternatively, RadA (not to be confused with the RadA recombinase of Archaea, a functional homologous of RecA) extends the D-loop even in the absence of RecA (21), and spontaneous annealing of the invading strand indirectly might facilitate the integration of heterologous sequences. Natural competent *Vibrio cholerae* or *Acinetobacter baylyi* cells, however, do not require RadA (referred to as RadA$_{Vch}$ and RadA$_{Aba}$) for efficient recombination of the internalized donor ssDNA with the homologous recipient genome during natural chromosomal transformation (22). Similarly, lack of *Escherichia coli* RadA (RadA$_{Eco}$) slightly impaired RecA$_{Eco}$-dependent Hfr conjugation, whose recombination intermediates are expected to be D-loop structures (23,24). It is likely, therefore, that the branch migration translocase used by bacteria of the Bacilli and γ-Proteobacteria Classes during genetic recombination are different ones. Similar discrepancies were observed when these cells were exposed to DNA damaging agents (18,23–26).

RadA, which is ubiquitous in bacteria, has four well-conserved motifs: a potential C4-type zinc-binding motif at the N-terminal domain, a central canonical RecA-like ATPase domain (H1-H4 motifs) and KNRFG motif, and the P/LonC domain at the C-terminus domain (18,20,23). A mutation at the Walker A (H1) or at the KNRFG motifs is dominant negative to RadA$_{Eco}$ or RadA/Sms alleles (18,24). These RadA$_{Eco}$ mutants fail to bind DNA, whereas the equivalent RadA/Sms mutant preferentially binds ssDNA or HJ DNA even in the apo form with similar affinity than *wt* RadA/Sms (18,21). The P/LonC domain of *Thermus thermophilus* RadA (RadA$_{Tth}$) and full-length RadA$_{Spn}$, which lack the serine–lysine protease catalytic dyad, adopt a dumbbell-shaped homohexameric structure homologue to that of the LonC protease (20,27). RadA$_{Spn}$ is functionally related to superfamily 4 (SF4) DNA helicases (20). As observed for hexameric DnaB-like helicases (28,29), RadA$_{Spn}$ or RadA/Sms unwinds DNA in the 5′→3′ direction (18,20). In contrast, RadA$_{Eco}$, which stimulates branch migration within the context of the RecA$_{Eco}$ filament, is unable to unwind a forked DNA substrate (21).

The average length of a RecA-mediated D-loop is ∼400-nucleotides (nt) (30–32), but the average size of donor ssDNA integration during natural transformation is ∼14,000-nt (33,34). It is likely that initial homologous pairing does not require a free end of the filament, and it can occur at any site along the RecA nucleoprotein filament; thus, a nascent and transient three-stranded non-interwound paranemic D-loop might be formed (Figure 1A) (30). However, if RadA binds to the 5′-tail of the 3′-invading strand, it would displace it, and thus reverse the transformation reaction; preventing recombination. To reconcile the observed RadA polarity with the assimilation of the incoming ssDNA, we have to assume that a RecA accessory protein or RecA itself might load RadA onto the recipient strands as depicted in Figure 1Aii (positions *a* and *b*) to facilitate the acquisition of the transforming ssDNA, as proposed (18,20). RecA bound to the displaced strand may recruit RadA/Sms to the invading strand, although this hypothesis is not further considered because RadA/Sms bound to the invading strand would displace it, preventing recombination. Alternatively, RecA assembled on the invading strand might load RadA/Sms onto the opposite strands as shown in Figure 1Aiv (positions *c* and *d*). If loading occurs at position *c*, the invading ssDNA would be displaced; behaving as an anti-recombinase during chromosomal transformation (Figure 1Av).

To explain that *Deinococcus radiodurans* RadA (RadA$_{Dra}$), in concert with RecA$_{Dra}$, contributes to facilitate extended synthesis-dependent strand annealing (SDSA) to reconstitute the bacterial genome disintegrated by ionizing radiation (35), we have to assume an alternative mechanism of RadA action. During double strand break (DSB) repair, after end processing, RecA filamented onto the 3′-tail of duplex DNA invades a homologous duplex, resulting in a plectonemic D-loop (30) (Figure 1Bi). RadA loaded onto the displaced strand and upstream of the invading end might extend the D-loop to facilitate replicase entry (to restore the genetic material lost by resection) and second-end capture (Figure 1Bii–iii, position *b*). Then, the resected second end anneals to the displaced strand of the D-loop, yielding an intermediate that could become in a double Holliday junction (HJ). In a second step, RadA/Sms loaded at positions *c* and *d* will contribute to disrupt the recombination intermediate to facilitate annealing of the displaced strands, leading to extended SDSA (Figure 1Biv–v). Thus, the loading step of RadA must be carefully tuned because recruitment to position *c* during chromosomal transformation shows an anti-recombination activity (Figure 1Av), but during DSB repair favours the SDSA pathway (Figure 1Bv).

In this study, using a combination of genetic and biochemical assays, we aim to decipher the role of RadA/Sms over the RecA-dependent reactions that take place during chromosomal transformation. We show that RadA/Sms variants with mutations in the C4 motif (*radA*13 [RadA/Sms C13A] and *radA*131 [RadA/Sms C13R]) fail to interact with RecA, but *wt* RadA/Sms or its mutant variant in the Walker A (*radA*1041 [K104R]) motif form a complex with RecA. RadA/Sms is crucial for chromosomal transformation, but is essential in the Δ*recG* background. The *radA*13 and *radA*131 mutations poisoned both chromosomal and plasmid transformation. Plasmid transformation is independent of RecA, but its absence suppresses the observed plasmid transformation defect in the *radA*131 context, suggesting that RadA/Sms may contribute to disassemble the dynamic RecA filament formed on heterologous plasmid DNA during plasmid transformation. *In vitro*, the RadA/Sms C13A and C13R variants preferentially bind ssDNA, albeit with lower efficiency than the *wt* protein. RadA/Sms C13A and C13R hydrolyse ATP in a
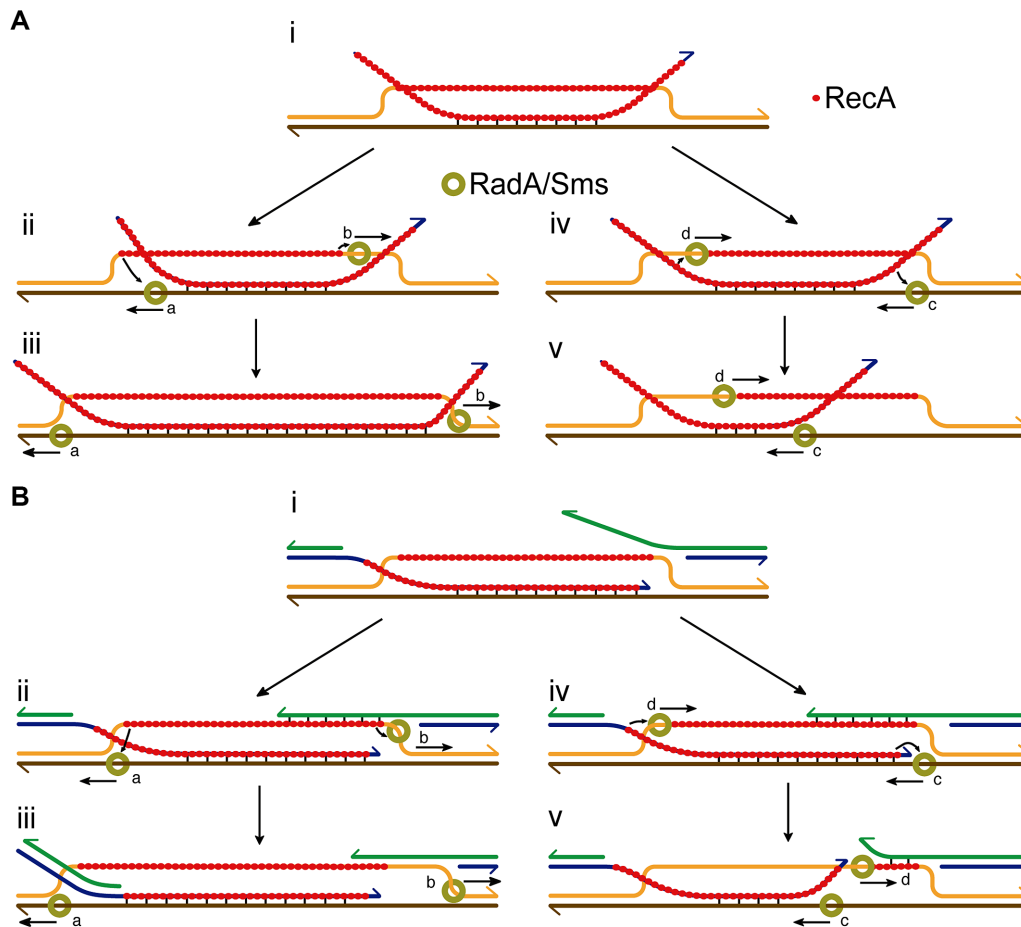
Figure 1. Proposed model for the action of the $5' \rightarrow 3'$ RadA/Sms helicase in coordination with RecA during natural transformation (**A**) and in DSB repair (**B**). RecA bound to the incoming linear ssDNA invades a homologous region of the chromosome forming a paranemic (A) or plectonemic D-loop (B). At the paranemic D-loop, RadA/Sms loaded at positions *a* and *b* divergently unwinds the substrates and might promote the integration of the transforming ssDNA (A, stages ii-iii). Alternatively, RadA/Sms can be loaded at positions *c* and *d*, and then, it disassembles the invading ssDNA or has no obvious effect (A, stages iv–v). During DSB repair, RadA/Sms loaded at positions *a* and *b* divergently unwinds the substrates, thereby facilitating the priming of DNA synthesis to restore the material lost by resection and with the capture of the second end (B, stages ii–iii). Alternatively, RadA/Sms can be loaded at positions *c* and *d*. Then, its helicase activity will disassemble the invading ssDNA substrate, and disengage the second end and thereby enhances synthesis-dependent strand annealing (B, stages iv–v).

ssDNA-dependent manner, but *wt* RadA/Sms does not. RadA/Sms C13A or C13R neither interacts with nor inhibits the ATPase activity of RecA, but *wt* RadA/Sms or a mutant variant in the Walker A domain inhibits the ATPase of RecA. RadA/Sms and its C13A or C13R variants unwind a 3′-fork DNA (a structure mimicking a replication fork with a fully synthesized leading-strand end and a gap in the lagging strand) in the $5' \rightarrow 3'$ direction (cognate substrate), but not the non-cognate 5′-fork DNA substrate (a structure mimicking a replication fork with a fully synthesized lagging-strand end and a gap in the leading strand). Addition of RecA, however, facilitates unwinding of non-cognate 5′-fork or D-loop substrates in the $5' \rightarrow 3'$ direction by RadA/Sms, but not by RadA/Sms C13A or C13R. Thus, we propose that RecA interacts with and loads RadA/Sms onto a D-loop and both proteins in concert facilitate homology-directed RecA-dependent integration of the internalized ssDNA during chromosomal transformation.

MATERIALS AND METHODS

Strains and plasmids

The *B. subtilis* BG214 (*trpC*E *metA*5 *amyE*1 *rsbV*37 *xre*1 *xkdA*1 *att*[SPβ] *att*[ICEBs1]) strain and its isogenic derivatives are listed in Supplementary Table S1. Codon 13, within the C4 motif (10-**C**X$_2$**C**GX$_7$G**XC**X$_2$**C**X$_2$W-30, underlined) was mutated. The *wt radA* TGC codon 13 coding for Cys, was exchanged for GCC or CGC, which encode for Ala or Arg, respectively, by site-directed mutagenesis, rendering the *radA*13 (C13A mutation) and *radA*131 (C13R mutation) genes. *Bacillus subtilis* BG214 cells bearing pBT61 were used to over-express the *recA* gene (36).

The DNAs of *wt radA*, *radA*13 or *radA*131 genes under the control of an IPTG-inducible promoter were used to transform and integrated into the *amyE* locus of competent *B. subtilis* BG1245 (*ΔradA*) cells (see Supplementary Table S1). The *ΔrecA* mutation was moved into the *ΔradA*

*radA*131 strain by chromosomal transformation (Supplementary Table S1).

A single C to T transition on codon 482 of the essential *rpoB* gene, which encodes for the β subunit of RNA polymerase, leads to the *rpoB*482 mutant that confers resistance to rifampicin (Rif^R). The *rpoB*482 DNA from different *Bacillus* species or subspecies (*B. subtilis* subsp. str. 168 *Bsu* 168 [*Bsu* 168, 99.96% sequence identity, 1 mismatch]; *B. subtilis* subsp. str. W23 [*Bsu* W23, 97.53%, 74 mismatches]; *B. atrophaeus* 1942 [*Bat* 1942, 91.65%, 250 mismatches]; *B. amyloliquefaciens* DSM7 [*Bam* DSM7, 89.88% 303 mismatches]; and *B. licheniformis* DSM13 [*Bli* DSM13, 85.48%, 435 mismatches] have been described (37,38) and were used to determine how sequence divergence affects the chromosomal transformation efficiencies. The dG + dC content of the different *rpoB*482 DNAs was $46.7 \pm 1.6\%$ and that of the recipient strain 45.3%. The sequence identity of the *Bacillus* RpoB protein in those variants ranged from 99.9% by the presence of the *rpoB*482 mutation down to 96% sequence identity. Oligomeric pUB110 DNA, which confers resistance to neomycin (Nm^R), was used for plasmid transformation assays (39).

Escherichia coli BL21(DE3)[pLysS] cells bearing pCB722 (*ssbA*), pCB1020 (*radA*) or pCB1036 (*radA*K104R) genes under the control of a rifampicin-resistant promoter (P_{T7}) were used to overproduce SsbA, RadA/Sms, and RadA/Sms K104R proteins, respectively, as described (13,18,26,40). The pCB1035-borne *radA* C13A and pCB1036 *radA* C13R genes were constructed in this study, and were used to overproduce RadA/Sms C13A or RadA/Sms C13R. *E. coli* BTH101 strain bearing the plasmids pUT18, pUT18C, pKT25 or pKNT25, with the T18 and T25 catalytic domains of the *Bordetella* adenylate cyclase gene (41) fused to *recA*, *radA*, *radA*13 or *radA*1041 genes, or the pKT25-zip and pUT18C-zip controls, were used for protein-protein interaction assays.

Transformation and survival assays

Natural competence development was carried out as described (42). Competent *B. subtilis* BG214 cells and its isogenic derivatives listed in Supplementary Table S1 were transformed with 0.1 μg/ml of *Bsu* 168 *rpoB*482 DNA (chromosomal transformation) or with pUB110 plasmid DNA (plasmid transformation). Chromosomal and plasmid transformants were selected plating on LB agar plates containing either Rif (8 μg/ml) or Nm (10 μg/ml) (42). The yield of Rif^R or Nm^R transformants was corrected for DNA uptake (assayed by determination of radioactively-labelled DNA uptake into cells grown to competence, measured by DNase I degradation of the DNA) and the rate of spontaneous mutations to Rif^R. Unless otherwise stated, the values obtained were normalised to that of the parental BG214 strain, which was considered 100 (42,43).

Competent *B. subtilis* BG1359 (Δ*rok*) cells and its isogenic derivatives listed in Supplementary Table S1 were transformed with *rpoB*482 DNA from different *Bacillus* species or subspecies with selection for Rif^R as described (37). The yield of Rif^R transformants was corrected as described above and normalized relative to the parental BG1359 strain, which was taken as 1 (42,43).

To measure the mean integration length, the chromosomal DNA of the Rif^R clones (*rpoB*482 transformants) was amplified by PCR and the resulting products were purified and sequenced to determine the integration end-points, and from them the mean integration length was calculated as described (38).

Methyl methanesulfonate (MMS), the UV radiation-mimetic 4-nitroquinoline-1-oxide (4NQO), mitomycin C (MMC) and H_2O_2 were from Sigma Aldrich. Cell sensitivity to chronic MMS, 4NQO, MMC or H_2O_2 exposure was determined by growing cultures to $OD_{560} = 0.4$, plating appropriate dilutions on LB agar plates supplemented with the indicated concentrations of the DNA-damaging agent, and measuring the number of viable colony-forming units measured. Plates were incubated overnight (16–18 h, 37°C) (44).

Enzymes, reagents, protein and DNA purification

All chemicals used were analytical grade. IPTG (isopropyl-β-D-thiogalactopyranoside) was from Calbiochem (Darmstadt, Germany), DNA polymerases, DNA restriction enzymes and DNA ligase were from New England Biolabs (Ipswich, MA, USA), and polyethyleneimine, DTT, ATP and dATP were from Sigma (Seelze, Germany). DEAE, Q- and SP-Sepharose were from GE Healthcare (Marlborough, MA, USA), hydroxyapatite was from Bio-Rad (Hercules, CA, USA), phosphocellulose was from Whatman (Kent, UK), and the Ni-column was from Qiagen (Hilden, Germany).

The proteins SsbA (18.7 kDa), RadA/Sms K104R and *wt* RadA/Sms (49.4 kDa), and RecA (38.0 kDa) were expressed and purified as described (7,12,18,45). RadA/Sms C13A and C13R were purified using the protocol developed for *wt* RadA/Sms (18). Purified SsbA, RecA, RadA/Sms and its mutant variants lack any protease, exonuclease or endonuclease activity in pGEM3 Zf(+) ssDNA or dsDNA in the presence of 5 mM ATP and 10 mM magnesium acetate (MgOAc). The corresponding molar extinction coefficients for SsbA, RadA/Sms and RecA were calculated as 11,400, 24,930, 22,350 and 15,200 M^{-1} cm^{-1}, respectively, at 280 nm, as described (45). Protein concentration was determined using the above molar extinction coefficients. RecA and RadA/Sms are expressed as moles of monomeric and SsbA as tetrameric protein. In this study, experiments were performed under optimal RecA conditions in buffer A (50 mM Tris–HCl pH 7.5, 1 mM DTT, 80 mM NaCl, 10 mM MgOAc, 50 μg/ml bovine serum albumin [BSA] and 5% glycerol), in which a single SSB tetramer binds in its fully wrapped (SSB_{65}) binding mode and all four subunits interact with ssDNA (46). RadA/Sms hexamer should bind ∼20-nt, and a RecA monomer should bind 3-nt (18,47).

The nucleotide sequence of the oligos used for constructing the DNA substrates is presented in Supplementary Material *Annex 1*, and the structures formed in Supplementary Figure S1. The oligos were annealed and the resulting products were gel purified (48–50) and stored at 4°C. DNA concentrations were established using the molar extinction coefficients of 8780 and 6500 M^{-1} cm^{-1} at 260 nm for ssDNA and dsDNA, respectively, and are expressed as moles of nt) or as moles of DNA molecules, as indicated.

Protein–protein interactions

In vivo protein–protein interactions were assayed using the adenylate cyclase-based bacterial two-hybrid technique (41,51). Plasmid-borne RadA/Sms, RadA/Sms C13A or RadA/Sms K104R fusions, at the N- and C-termini of the T18 or T25 catalytic domain, were co-transformed with plasmid-borne RecA fusions, at the N- and C-termini of the T18 catalytic domain, into the reporter BTH101 strain. The empty vectors or the pKT25-zip and pUT18C-zip vectors were co-transformed into the reporter strain as negative and positive controls, respectively. Different dilutions were spotted onto LB plates supplemented with ampicillin, kanamycin, streptomycin, 0.5 mM IPTG and 10% X-gal (Figure 3A–C). The plates were then incubated at 25°C for 3–4 days. Each transformation was performed at least in triplicate and a representative result is shown.

In vitro protein–protein interactions were assayed using affinity chromatography. His-tagged RadA/Sms (*wt* or C13A) (1.5 µg) or RecA (1.5 µg) alone or His-RadA/Sms (*wt* or C13A) mixed with RecA (1.5 µg each), in the presence or absence of ssDNA and ATP, were loaded onto a 50-µl Ni²⁺ microcolumn at room temperature in Buffer B (50 mM Tris–HCl pH 7.5, 10 mM MgCl₂ and 5% glycerol) containing 80 mM NaCl and 20 mM imidazole. When indicated, buffer B additionally contained 5 mM ATP and 10 µM pGEM3 Zf(+) ssDNA. After extensive washing, the retained proteins were eluted with 50 µl of Buffer B containing 80 mM NaCl and 400 mM imidazole. The proteins were separated by 17.5% SDS-PAGE, gels were stained with Coomassie Blue or alternatively proteins were detected using anti-His-tag monoclonal and anti-RecA-polyclonal antibodies by western blotting.

Protein–DNA interactions

For the electrophoretic mobility shift assay (EMSA) studies, DNA substrates were first assembled by annealing different oligonucleotides, as represented in Supplementary Material *Annex* 1 and Supplementary Figure S1, with one of the oligonucleotides radiolabelled. Typically, [γ³²P]-substrate DNA was incubated with different amounts of proteins for 15 min at 37°C in buffer C (50 mM Tris–HCl pH 7.5, 50 mM NaCl, 10 mM MgOAc, 1 mM DTT, 5% glycerol and 50 µg/ml BSA) in a 20-µl final volume, as described in the Figure legend. Prior to addition of loading buffer (1 mM EDTA, 0.1% bromophenol blue and 0.1% xylene cyanol), 0.1% glutaraldehyde was added and the samples were subjected to 6% PAGE. Gel electrophoresis was conducted either using 0.25× or 1× Tris–borate–EDTA (TBE) as running buffer, at 180 V and room temperature, and the gels were dried prior to phosphorimaging analysis. Phosphorimager screens were analysed using a Personal Molecular Imager system and the Quantity One software (Bio-Rad) to obtain apparent binding constant (K_{Dapp}) values.

ATP hydrolysis assays

The ATP hydrolysis activity of the RadA/Sms protein was assayed *via* a NAD/NADH coupled spectrophotometric enzymatic assay (7). The rate of RadA/Sms-mediated ATP hydrolysis was measured in buffer A containing 5 mM (d)ATP (for 30 min at 37°C) (7). The order of addition of circular 3199-nt pGEM3 Zf(+) ssDNA (cssDNA), poly(dT) ssDNA, poly(dA) ssDNA, 3′-tailed DNA or 5′-tailed DNA (10 µM in nt), linear 3199-nt pGEM3 Zf(+) dsDNA (lds-DNA) or HJ DNA (20 µM in nt) and purified proteins is indicated in the text. Data obtained from A_{340} absorbance were converted to (d)ADP produced, and plotted as a function of time (51).

DNA helicase assays

The different DNA substrates (see Supplemental material *Annex 1*, Supplementary Figure S1) used were incubated with increasing concentrations of RadA/Sms or its mutant variants, or RecA, for 15 min at 30°C in buffer A containing 2 mM ATP in a 20-µl volume, as previously described (40). The reactions were deproteinised by phenol–chloroform, DNA substrates and products were precipitated by NaCl and ethanol addition, and subsequently separated using 10% (w/v) PAGE. Gels were run and dried prior to phosphorimaging analysis, as described above.

RESULTS

RadA/Sms is essential for chromosomal transformation in Δ*recG* cells

Previous assays have shown that RadA/Sms is crucial, and RecA is essential for natural chromosomal transformation, but in their absence plasmid transformation is marginally affected if at all (Supplementary Material, *Annex* 2, Figure 2A) (18,42). Since the DNA uptake machinery takes any DNA with similar efficiency, and competent Δ*radA* and Δ*recA* cells are reduced and blocked in chromosomal transfomation, but proficient in plasmid transformation, we concluded that RecA and RadA/Sms are involved in HR rather than in competence development, DNA uptake or controlling the competence exit (18,47), and assumed that another function contributes to chromosomal transformation in the Δ*radA* context.

As described in Supplementary Material, *Annex 2*, lack of RecG or RuvAB marginally reduced chromosomal and plasmid transformation, when compared with competent *rec⁺* cells (Figure 2A). Inactivation of *B. subtilis ruvAB* is synthetically lethal in the Δ*recG* background (44,52). To study which other branch migration translocase can contribute to natural chromosomal transformation in the Δ*radA* background, combinations of Δ*radA* with null mutants in the other two branch migration translocases (RuvAB or RecG) were tested.

Competent Δ*recG* Δ*radA* and Δ*ruvAB* Δ*radA* cells, as well as the Δ*recA* control, were transformed with chromosomal and plasmid DNA (Supplementary Material, *Annex 2*). The chromosomal transformation frequencies of competent Δ*ruvAB* Δ*radA* cells were similar to the ones in single Δ*radA* cells (Figure 2A). This is consistent with the observation that chromosomal transformation involves a three-strand exchange reaction and the formation of a D-loop intermediate, whereas RuvABencircles two duplex arms and translocates HJ structures (53–55).

As shown in Supplementary Material, *Annex 2*, competent Δ*radA* Δ*recG* cells were blocked in chromosomal trans-

A

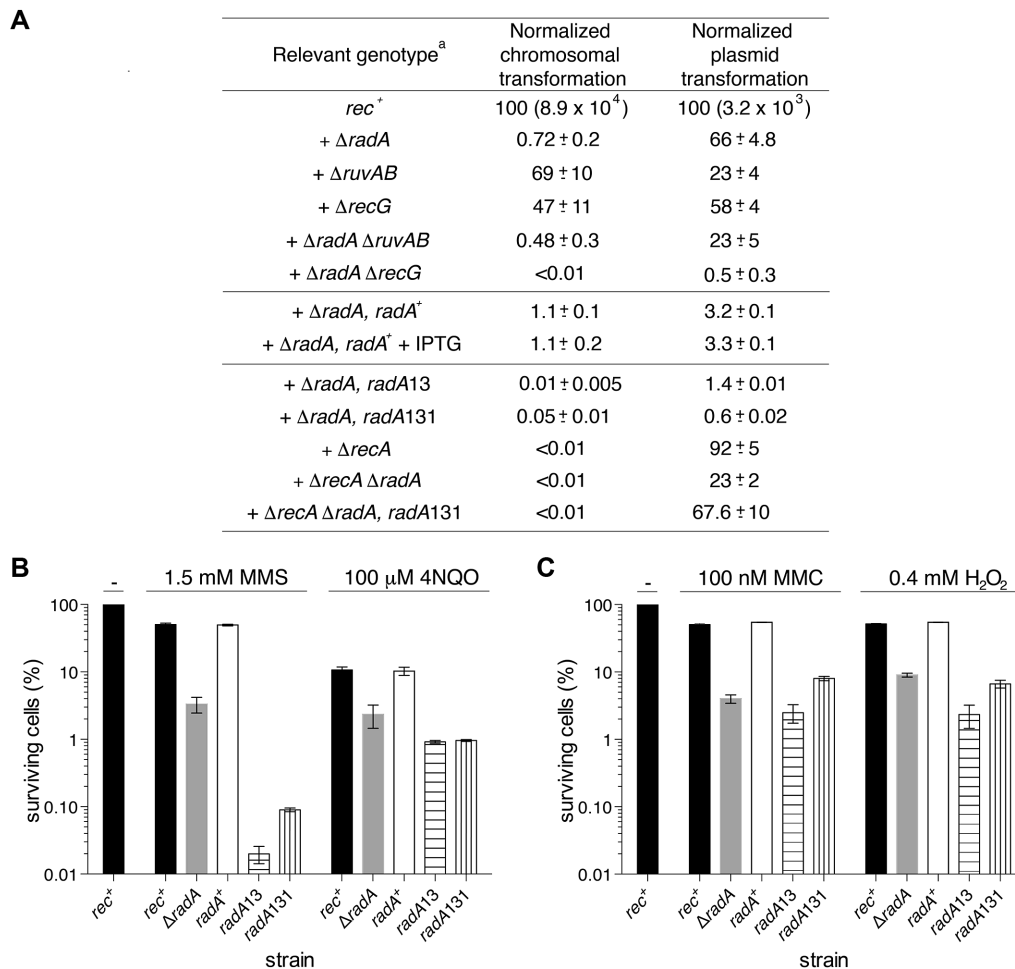| Relevant genotype[a]	Normalized chromosomal transformation	Normalized plasmid transformation
rec[+]	100 (8.9 x 10^{4})	100 (3.2 x 10^{3})
+ Δ*radA*	0.72 ± 0.2	66 ± 4.8
+ Δ*ruvAB*	69 ± 10	23 ± 4
+ Δ*recG*	47 ± 11	58 ± 4
+ Δ*radA* Δ*ruvAB*	0.48 ± 0.3	23 ± 5
+ Δ*radA* Δ*recG*	<0.01	0.5 ± 0.3
+ Δ*radA, radA*[+]	1.1 ± 0.1	3.2 ± 0.1
+ Δ*radA, radA*[+] + IPTG	1.1 ± 0.2	3.3 ± 0.1
+ Δ*radA, radA*13	0.01 ± 0.005	1.4 ± 0.01
+ Δ*radA, radA*131	0.05 ± 0.01	0.6 ± 0.02
+ Δ*recA*	<0.01	92 ± 5
+ Δ*recA* Δ*radA*	<0.01	23 ± 2
+ Δ*recA* Δ*radA, radA*131	<0.01	67.6 ± 10

Figure 2. Genetic analysis of RadA/Sms mutant variants. (**A**) The role of RadA/Sms in chromosomal and plasmid transformation. Competent *B. subtilis* cells were transformed with 0.1 μg of *rpoB*482 DNA (Rif[R]) or pUB110 plasmid DNA (Nm[R]). The yield of Rif[R] (chromosomal transformation) and Nm[R] transformants (plasmid transformation) was normalized relative to that of the *rec*[+] strain, recorded as 100 (in parentheses, number of transformants per 0.1 μg DNA/ml). The results are shown as mean ± SEM of at least four independent experiments. Survival of mutant strains upon chronic exposure to MMS and 4NQO (**B**), or to MMC and H₂O₂ (**C**). The *rec*[+] (BG214), Δ*radA* (BG1245), Δ*radA radA*[+] (BG1601), Δ*radA radA*13 (BG1589) and Δ*radA radA*131 (BG1591) cells were grown to reach exponential phase (OD₅₆₀ = 0.4) in LB medium at 37°C, serially diluted, and then 10 μl of serial 10-fold dilutions were spotted on LB plates containing the indicated concentration of the denoted drug or in its absence (–). Plates were incubated overnight at 37°C, and colonies were counted from appropriate dilutions. Results are the mean ± SEM of >3 independent experiments.

formation and strongly impaired in plasmid transformation (Figure 2A). It is likely that RadA/Sms and RecG process D-loop intermediates differently, and RadA/Sms is the prominent DNA translocase during chromosomal transformation. This is consistent with the fact that a 3′ leading end fork is an isomer of a D-loop, and monomeric RecG processes forked structures, and converts them into HJ structures in a 3′→5′ direction (54–56).

A RadA/Sms C4 mutation impairs chromosomal and plasmid transformation

To determine whether the C4 motif of the 458-amino acids long RadA/Sms protein contributes to natural transformation, the *wt radA* (*radA*[+]), *radA*13 (C13A mutation) and *radA*131 (C13R) genes (see Material and methods), under the control of an IPTG-inducible promoter, were ectopically integrated into the *amyE* locus of the marker-less Δ*radA* strain. The ectopic integration was performed to avoid any

negative effect on downstream genes (namely *disA*, and stress response *yacL* gene) that could potentially occur if integrated into the native locus.

Basal expression of the *radA*[+] gene was sufficient to complement the Δ*radA* defect in response to DNA damage, but expression of the *radA*13 or *radA*131 mutant genes failed to complement the Δ*radA* defect in response to the different DNA damaging agents tested in the presence or the absence of IPTG (Figure 2B and C). As shown in Supplementary Material, *Annex 3*, the *radA*13 and *radA*131 cells were more sensitive to 1.5 mM MMS and 100 μM 4NQO when compared with the Δ*radA* control (Figure 2B). These results suggest that a single copy of the *radA*13 or *radA*131 gene negatively interferes with DNA repair. Similarly, the *radA*_*Eco* C28Y allele (*radA*100), in the C4 motif, produces a dominant-negative phenotype (16,24).

To examine the role of the *radA*13 and *radA*131 mutations on natural transformation, cells were made competent
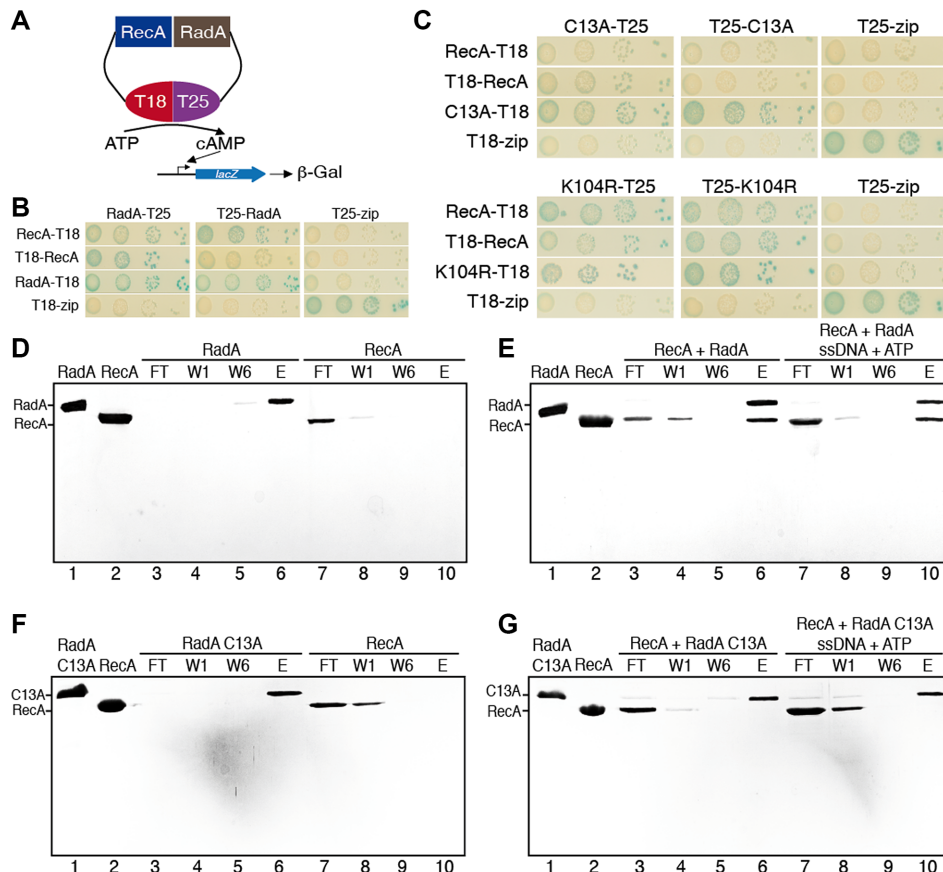
Figure 3. RadA/Sms C13A interacts with itself but does not interact with RecA. (**A**) Scheme of the bacterial two-hybrid system used. *E. coli* BTH101 cells expressing RadA/Sms, RadA/Sms C13A, RadA/Sms K104R or RecA fused to either the T18 or T25 domain of the *Bordetella* adenylate cyclase, were tested. (**B** and **C**) Dilutions of the indicated combinations of co-transformed BTH101 cells on plates supplemented with IPTG and X-gal were analysed. The appearance of blue colour in the colony due to the breakdown of X-gal in the medium was considered as a positive interaction. As a control, the *E. coli* Zip protein fused to T18 or T25 domain was used to score for positive interactions and rule out false positive interactions. (**D–G**) The interaction of RecA with RadA/Sms or RadA/Sms C13A was analysed by affinity chromatography. His-tagged RadA/Sms (D), His-tagged RadA/Sms C13A (F) or RecA were incubated with 50 μl of the Ni^{2+} matrix in buffer B containing 80 mM NaCl and 20 mM imidazole, and the flow-through (FT) was collected. The Ni^{2+} matrix was washed (W) six times with 500 μl of the same buffer (the first [W1] and the last [W6] are shown). Bound His-tagged RadA/Sms or C13A was eluted (E) with buffer B containing 80 mM NaCl and 400 mM imidazole. (**E** and **G**) RecA and His-tagged RadA/Sms or His-tagged RadA/Sms C13A were incubated with 50 μl of the Ni^{2+} matrix in buffer B supplemented with 80 mM NaCl lacking (lanes 3–6) or containing 10 μM ssDNA and 5 mM ATP (lanes 7–10), and the FT was collected. The Ni^{2+} matrix was washed and proteins were eluted. The collected protein fractions were separated by 17.5% (w/v) SDS-PAGE. The position(s) of the RadA/Sms, its mutant C13A and RecA proteins is(are) indicated.

and the frequency of chromosomal and plasmid transformation was analysed. Unexpectedly, competent *radA*$^+$ cells were marginally affected on chromosomal, but impaired in plasmid transformation in the Δ*radA* context (Figure 2A), suggesting that the *radA*$^+$ gene, in the presence or absence of IPTG, did not complement the Δ*radA* defect (Figure 2A). It is likely that repair-by-recombination is less sensitive to the RadA/Sms levels (see *Annex 3*, Figure 2B and C) than the genetic recombination machinery.

The *radA*13 or *radA*131 mutation reduced the chromosomal transformation frequency by ∼70-fold and ∼15-fold, and the plasmid transformation by ∼50- and ∼110-fold, respectively, when compared with the competent Δ*radA* control (Figure 2A). Similar results were observed in the presence of IPTG in the *radA*13 and *radA*131 strains (data not shown), suggesting that the RadA/Sms C13A and C13R mutations poisoned chromosomal, and strongly affected the plasmid transformation frequency.

Cross-talks between RadA/Sms and RecA are necessary for plasmid transformation

The *radA* gene is epistatic to the *recA* gene in response to DNA damage (26,57). RecA is apparently dispensable for oligomeric plasmid transformation, but the RecA nucleoprotein filaments formed on the internalised heterologous plasmid ssDNA impair plasmid transformation if such RecA filaments fail to be disassembled (58,59). To test whether RadA/Sms C13A or C13R contributes to the processing of RecA intermediates the Δ*recA* mutation was moved onto the *radA*131 background, and as control in the Δ*radA* strain. As expected, the absence of RecA blocks chromosomal transformation, but it is dispensable for plasmid transformation (Figure 2A). The absence of RecA suppressed the plasmid transformation defect in the competent *radA*131 cells (Figure 2A) when compared with the Δ*radA* strain, suggesting that the plasmid transformation defect is overcome by deleting RecA. Unexpectedly, com-

petent $\Delta recA$ $\Delta radA$ cells were also marginally impaired in plasmid transformation when compared to the single parents (Figure 2A), suggesting that inactivation of *radA* directly or indirectly impairs plasmid transformation in the $\Delta recA$ context.

RecA physically interacts with RadA/Sms (Figure 3B and D-E) (18). We have tested whether different RadA/Sms mutants interact with RecA. As revealed in Supplemental material, *Annex 4*, the RadA/Sms K104R mutant, which cannot bind ATP, physically interacts with itself and with RecA (Figure 3C). The RadA/Sms C13A protein interacted with itself, but it did not form a complex with RecA *in vivo* or *in vitro* (Figure 3C and F–G). RadA/Sms C13A failed to interact with RecA even in the presence of ssDNA and ATP (Figure 3G). From these results and the genetic analysis of the mutants, we propose that *wt* RadA/Sms contributes to destabilise the RecA nucleoprotein filament formed on the heterologous plasmid ssDNA to facilitate the role of the RecA modulators RecX and/or RecU, but the RadA/Sms variants in the C4 motif might not be able to facilitate the disassembly of RecA from the plasmid ssDNA during plasmid transformation (see Figure 2A) (58,59).

RadA/Sms C13A or C13R preferentially binds ssDNA

To understand how the RadA/Sms mutant variants in the C4 domain interact with different DNA substrates, *wt* RadA/Sms and its mutant variants C13A or C13R were purified and used in EMSA experiments. Increasing concentrations of RadA/Sms and its mutant variants were incubated with $[\gamma^{32}P]$-radiolabelled ssDNA, dsDNA or HJ DNA (1 nM in DNA molecules) (Supplemental material, *Annex 1* and described in Supplementary Figure S1). In the absence of a nucleotide cofactor, RadA/Sms C13A or C13R preferentially bound ssDNA, followed by HJ DNA and then dsDNA (Supplementary Figure S2). Nevertheless, RadA/Sms C13A or C13R mutant variants bound to the different DNA substrates with lower affinity than the apo *wt* RadA/Sms protein (Supplementary Figure S2B) (18).

RadA/Sms C13A and C13R mutants hydrolyse ATP in a ssDNA-dependent manner

In the presence or absence of cssDNA, the maximal rate of ATP hydrolysis of *wt* RadA/Sms was similar (catalytic rate constant [k_{cat}] of $\sim$9.7 min^{-1}) (Figure 4A, Supplementary Table S2) (18). The rate of ATP hydrolysis by RadA/Sms correlated with the protein amount under most conditions (RadA/Sms 400 or 800 nM) (Figure 4A, Supplementary Table S2), suggesting that *wt* RadA/Sms-mediated ATP hydrolysis is not stimulated by addition of cssDNA.

In the absence of cssDNA, RadA/Sms C13A or C13R hydrolysed ATP with a k_{cat} of $\sim$9.6 and $\sim$9.7 min^{-1}, respectively, but in the presence of cssDNA, the ATPase activity of the RadA/Sms C13A and C13R mutants increased $\sim$5-fold (Figure 4A and Supplementary Figure S3A, Table S2). These results suggest that the integrity of the C4 motif is not necessary for ssDNA-dependent ATP hydrolysis. The structure of the zinc-binding C4 motif is undefined (20), but it could be predicted that the C4 mutants undergo structural transitions that upon binding to cssDNA show their maximal rate of ATP hydrolysis. In other words, *wt* RadA/Sms

may need to be activated by an unknown factor, which directly or indirectly acts with the C4 domain, to become a ssDNA-dependent ATPase.

RadA/Sms C13A and C13R mutants bind natural ssDNA and partially displace SsbA

To further explore the stimulation of the ATPase activity of RadA/Sms C13A or C13R, several DNA substrates were used as putative effectors. RadA/Sms C13A or C13R bound to natural linear 80-nt ssDNA (lssDNA) hydrolyzed ATP with similar efficiency than cssDNA (Supplementary Table S2). When the 80-nt lssDNA was replaced by an unstructured 80-nt long poly(dT) or poly(dA) lssDNA, however, the maximal rate of ATP hydrolysis was reduced to levels comparable with the absence of lssDNA (Figure 4B and Supplementary Figure S3B, Table S2). It is likely that the RadA/Sms variants might bind to regions with secondary structure or ssDNA–dsDNA junctions. To address this question short substrates having 3′ or 5′ overhangs were used. RadA/Sms C13A or RadA/Sms C13R bound to 40-nt long 3′-tailed or 5′-tailed duplex substrates hydrolysed ATP with a similar k_{cat} than when bound to 80-nt long lssDNA or cssDNA (Figure 4B and Supplementary Figure S3B, Table S2). To confirm if RadA/Sms variants bind to ssDNA containing secondary structures (or ssDNA-dsDNA junctions), the cssDNA was pre-incubated with a stoichiometric SsbA concentration, a protein that removes secondary structures from ssDNA (46). In the presence of SsbA (1 SsbA tetramer/33-nt), RadA/Sms C13A- or C13R-mediated ATP hydrolysis was still stimulated by the presence of cssDNA, but the maximal rate of ATP hydrolysis of these mutant variants was decreased by $\sim$2-fold (k_{cat} $\sim$21 and $\sim$22 min^{-1}) (Figure 4A and Supplementary Figure S3A, Table S2), suggesting that RadA/Sms may not bind to secondary structures, but SsbA may compete with RadA/Sms C13A or C13R mutant variants for ligand binding.

When the cssDNA was replaced by linear dsDNA (ldsDNA) or HJ DNA the maximal rate of RadA/Sms C13A- or C13R-mediated ATP hydrolysis was only stimulated by $\sim$2- and $\sim$1.4-fold, respectively (Figure 4A and Supplementary Figure S3A, Table S2). The understanding of the lack of stimulation of their ATPase activity by poly(dT) or poly(dA) ssDNA, however, will require structural analysis of RadA/Sms C13A in the presence of various ssDNA substrates.

RadA/Sms inhibits the ATPase activity of RecA

RadA$_{Spn}$ is functionally related to DnaB-like DNA helicases (20). A helicase loader interacts with and recruits its cognate DnaB-like helicase, but it inhibits its activities (29). Then, a third protein, the DNA primase, has to interact with the loader-helicase complex to release it from its loader and to activate helicase unwinding of DNA substrates having a 5′-tail and a 3′-ssDNA overhang (60,61). RecA interacts with RadA/Sms or RadA/Sms K104R, but not with RadA/Sms C13A (Supplemental material, *Annex 4*, Figure 3). To test whether RecA loads RadA/Sms onto ssDNA, we employed the hydrolysis of ATP as an indirect measurement of protein recruitment.
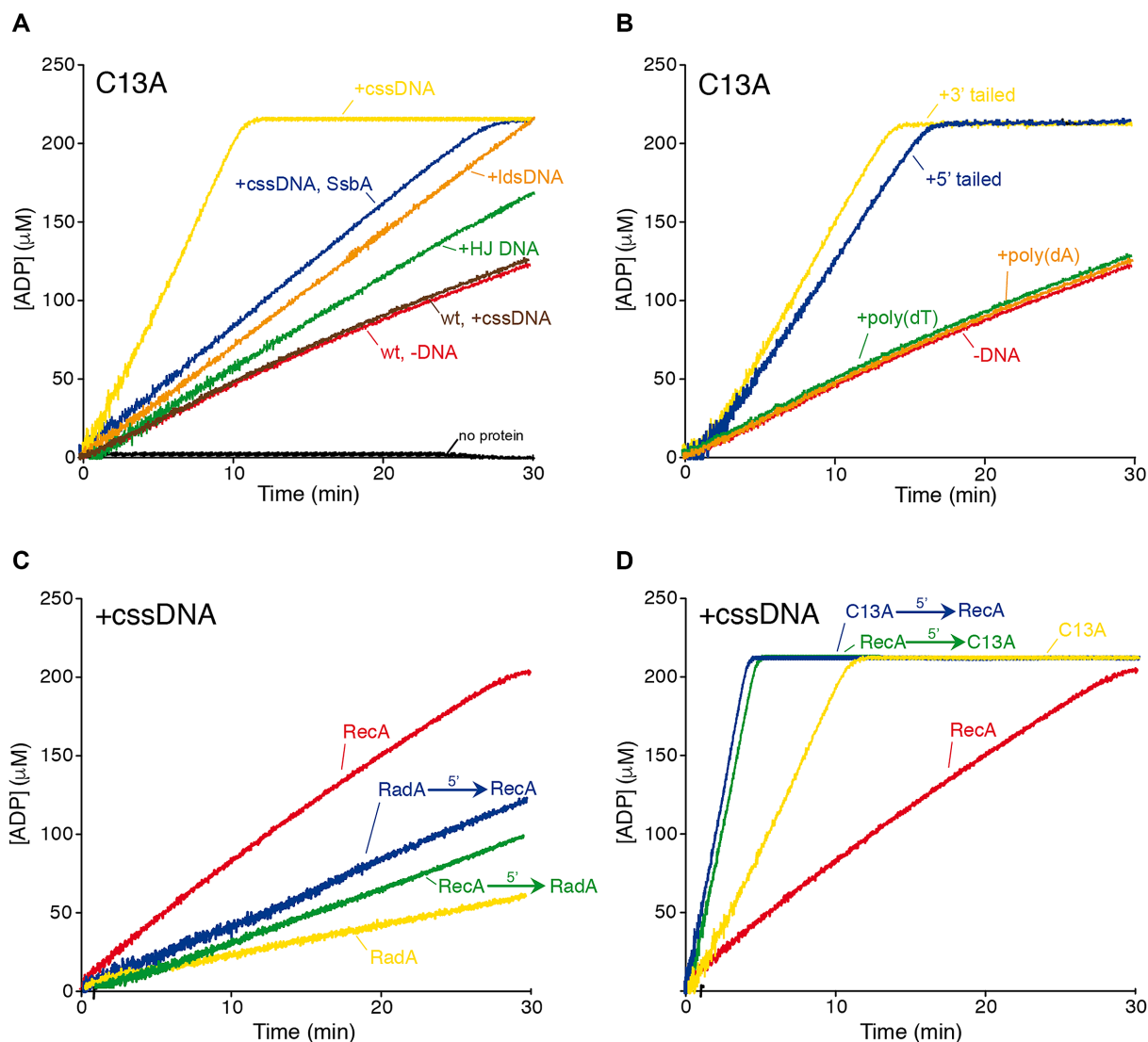
Figure 4. RadA/Sms C13A preferentially hydrolyses ATP in the presence of ssDNA. (**A**) RadA C13A (400 nM) was incubated with or without the indicated DNA (cssDNA [at 10 μM in nt], HJ DNA or ldsDNA [at 20 μM in nt]) in buffer A containing 5 mM ATP (5 min, 37°C) and then ATPase activity was measured for 30 min. In reactions with SsbA, the cssDNA was pre-incubated with SsbA (300 nM) (5 min, 37°C), then RadA/Sms C13A was added and the ATPase activity was measured. For comparison, the ATPase activity of *wt* RadA/Sms (400 nM) with (brown line) or without (red line) cssDNA is shown. The black line is a control reaction corresponding to an ATPase assay in the absence of RadA/Sms (*wt* or C13A). (**B**) RadA C13A (400 nM) was incubated with or without the indicated DNA (poly(dT) ssDNA, poly(dA) ssDNA, 3'-tailed or 5'-tailed duplex at 10 μM in nt) in buffer A containing 5 mM ATP (5 min, 37°C) and then ATPase activity was measured for 30 min. (**C-D**) RecA (800 nM) or *wt* (**C**) or RadA/Sms C13A (**D**) (200 nM) was pre-incubated with cssDNA (10 μM, in nt) (5 min, 37°C). Then, *wt* (**C**) or RadA/Sms C13A (**D**) or RecA was added, and the ATPase activity was measured. The order of protein addition is indicated. Representative graphs are shown here, and quantification of ATP hydrolysed is shown as the mean of >3 independent experiments in Supplementary Table S2.

At least three types of mechanisms for RadA/Sms loading can be envisioned. First, a RecA nucleoprotein filament loads RadA/Sms onto cssDNA but the ATPase activity is lower than the sum, suggesting that one of them is inactivated. Second, RecA loads RadA/Sms onto cssDNA and promotes a structural transition in RadA/Sms to make it a ssDNA-dependent ATPase, thus the combined RecA- and RadA/Sms-mediated ATP hydrolysis may be higher than the sum of their independent activities. Finally, RecA transiently interacts with and loads RadA/Sms onto cssDNA, and the ATPase activity is proximal to the sum of their independent activities if such RadA/Sms activation does not occur.

Accepting that both enzymes operate mostly under steady-state conditions, the maximal number of substrate-to-product conversion per unit of time for a 1 μM enzyme (k_{cat}) was measured. RecA (800 nM, 1 RecA monomer/12-nt) bound to the 3199-nt cssDNA quickly hydrolyzed ATP at a rate near to the formerly observed k_{cat} of 9.6 ± 0.4 min^{-1}, and RadA/Sms (200 nM, 1 RadA/Sms monomer/50-nt) hydrolysed ATP with a k_{cat} of 9.5 ± 0.1 min^{-1} (Figure 4C), thus both hydrolyzed ATP with similar k_{cat} (Figure 4C).

RadA/Sms was pre-incubated with cssDNA (5 min at 37°C), then RecA was added (at a RecA:RadA/Sms ratio, 4:1) and the ATPase activity was measured. Unexpectedly, RecA incubated with the preformed RadA/Sms–ssDNA complex reduced the maximum rate of ATP hydrolysis, k_{cat} of ∼4.1 min^{-1}. When the cssDNA was preincubated with RecA, and then RadA/Sms was added, the maximal rate of ATP hydrolysis was further decreased (k_{cat} ∼ 3.4 min^{-1}) (Figure 4C, Supplementary Table S2), suggesting that the ATPase activity of both proteins decline.

RadA/Sms might compete with RecA for ssDNA binding (Figure 4C and Supplementary Figure S2). To test that, RadA/Sms was replaced by the RadA/Sms C13A mutant, which fails to interact with RecA (Figure 3). When bound to ssDNA, RecA and RadA/Sms C13A alone hydrolyse ATP with a k_{cat} of 9.6 ± 0.4 min^{-1} and 48.5 ± 0.7 min^{-1}, respectively (Figure 4D, Supplementary Table S2). The maximal rate of ATP hydrolysis of RecA and of the preformed RadA/Sms C13A-cssDNA complex approached the sum of their independent activities (k_{cat} ∼55.1 min^{-1}) (Figure 4D, Supplementary Table S2). Similarly, when the RecA nucleoprotein filaments were pre-incubated with cssDNA and then RadA/Sms C13A was added, the maximal rate of ATP hydrolysis of both proteins was about the sum of their independent activities (k_{cat} ∼54.2 min^{-1}) (Figure 4D, Supplementary Table S2), indicating that RadA/Sms C13A and RecA bound cssDNA independently, and their combined rate of ATP hydrolysis can be measured. It is likely that one enzyme interacts with and reduces the ATPase activity of the other, but in the absence of such protein-protein interaction the ATP hydrolysis rate of both ATPases is not affected. To further analyse this negative effect, *wt* RadA/Sms was replaced with a catalytically inactive Walker A mutant, RadA/Sms K104R, unable to bind and hydrolyse ATP (18), but still able to interact with RecA (Figure 3). At a 0.25:1 RadA/Sms K104R:RecA ratio, RadA/Sms K104R inhibited the maximal rate of RecA-mediated ATP hydrolysis (Supplementary Figure S3C), suggesting that RadA/Sms K104R interacts with and inhibits the ATPase activity of RecA. It is likely that RadA/Sms interacts in a functionally significant manner with a RecA filament, and reduces its ATPase activity (see below).

RadA/Sms unwinds a 5′-tailed but not a 3′-tailed duplex substrate

A hexameric DnaB-like DNA helicase cannot unwind a 5′-tailed duplex substrate because the duplex DNA passes through the central channel, but it unwinds replication fork-like structures (i.e. 5′-tailed duplex with a 3′-ssDNA overhang) with a 5′→3′ polarity (60,62). To test whether *wt* RadA/Sms and its mutant variants C13A or C13R can unwind tailed duplex substrates or if they require substrates that mimic replication forks, two different radiolabelled substrates (5′- or 3′-tailed duplex, Supplementary Figure S1) lacking a complementary overhang were used for DNA unwinding assays (Supplementary Figure S4, the asterisk denotes the labelled 5′-end).

Increasing RadA/Sms C13A or RadA/Sms C13R concentrations unwound the 5′-tailed duplex substrate with analogous efficiency, and similar to *wt* RadA/Sms (Supple-

mentary Figure S4, C and E, lanes 5–7). This indicates that the *wt* RadA/Sms and its mutant variants bound to the 5′-tail and unwound the duplex substrate in the 5′→3′ direction, in spite of the absence of a 3′-ssDNA overhang. In contrast, RadA/Sms C13A, RadA/Sms C13R or *wt* RadA/Sms did not unwind a 3′-tailed duplex DNA (Supplementary Figure S4B, D and F, lanes 3–7). Since both 3′- and 5′-tailed duplex substrates stimulate the ATPase activity of RadA/Sms C13A or C13R (Figure 4B), we assume that the protein binds and translocates on the 3′-tail of the duplex substrate in an orientation-specific manner. Thus, if RadA/Sms tracks along the 3′-tail of the substrate in the 5′→3′ direction, it should move away from the junction, failing to unwind the 3′-tailed duplex substrate.

RadA/Sms unwinds a 3′-tailed substrate in the presence of RecA

To test whether RecA loads RadA/Sms onto ssDNA and stimulates unwinding, and if RecA-mediated loading imposes a polarity to RadA/Sms, we performed unwinding assays with the 5′- or 3′-tailed duplex substrates with a fixed RadA/Sms and increasing RecA concentrations. RecA·ATP polymerizes onto the ssDNA in the 5′→3′ direction and towards the ssDNA-dsDNA junction on the 5′-tailed duplex or away from the junction on the 3′-tailed duplex (30–32). In the absence of complementary ssDNA, RecA·ATP failed to unwind the short tailed duplex substrates (Supplementary Figure S4A-B, lane 10) (30–32).

At a low RecA:RadA/Sms ratio (0.4:1), RadA/Sms and its mutant variants unzipped the 5′-tailed substrate with a similar efficiency than in the absence of RecA (Supplementary Figure S4A, C and E, lanes 11 versus 12). At RecA:RadA/Sms ratios of 0.8:1 or higher, however, RadA/Sms unwound this substrate with lower efficiency (Supplementary Figure S4A, lanes 11 versus 13–15). A similar result was observed when RadA/Sms was replaced by RadA/Sms C13A or C13R (Supplementary Figure S4C and E, lanes 11 versus 14–15). From these results it can be inferred that: (i) RecA polymerised on the 5′-tail towards the ssDNA-dsDNA junction (in the 5′→3′ direction) might partially compete with RadA/Sms or RadA/Sms variants for ssDNA binding; (ii) the reduction in the ATP hydrolysis rate of the RecA-ssDNA-RadA/Sms complex (see Figure 4C) cannot explain the inhibition of unwinding, because RadA/Sms C13A or C13R and RecA show normal rates of ATP hydrolysis and (iii) a 3-fold excess of RecA reduces but does not inhibit the unwinding activity of RadA/Sms. It is likely that RadA/Sms partially displaces RecA from the ss-DNA.

Unexpectedly, RadA/Sms unwound the 3′-tailed duplex DNA substrate in the presence of RecA (Supplementary Figure S4B, lanes 11 versus 13–15), suggesting that RecA interacts with and promotes recruitment of RadA/Sms on the non-cognate DNA substrate, and then RadA/Sms unwinds it. A RecA·ATP filament formed in the 3′-tailed duplex substrate, however, was unable to activate the RadA/Sms C13A or C13R mutant to unwind the non-cognate DNA substrate (Supplementary Figure S4D and F, lanes 12–15), suggesting that a RecA-RadA/Sms interaction is necessary and sufficient to activate the unwinding of the non-cognate DNA

substrate. Intriguingly, RecA$_{Spn}$ fails to stimulate RadA$_{Spn}$ unwinding of the 3′-tailed duplex substrate (20).

An interaction of RadA/Sms with the 3′-end of the RecA nucleoprotein filament should load RadA/Sms on the same strand and away from the ssDNA-dsDNA junction, causing no effect on helicase activity over this substrate. We can envision that RecA disassembly might facilitate the spontaneous thermal fraying of the complementary strand. Then, the interaction of the 5′-end of a RecA·ATP filament with RadA/Sms loads it at the fraying in the complementary strand on the opposite strand, with RadA/Sms unwinding this DNA substrate in the in the 5′→3′ direction. The RadA/Sms translocation step size remains undefined.

RadA/Sms unwinds forked DNA in the 5′→3′ direction

To understand how RadA/Sms unwinds both the cognate and non-cognate substrates, a 3′-fork DNA (a replication fork with a fully synthesised leading-strand end and a gap in the lagging strand [or 5′-flap DNA], schematised in Figure 5A, C and Supplementary Figure S1) or a 5′-fork DNA (a replication fork with a a fully synthesised lagging-strand end and a gap in the leading strand [3′-flap DNA], schematised in Figure 5B, D and Supplementary Figure S1) were used.

RadA/Sms bound to the 5′-tail of the 3′-fork substrate unwound the radiolabelled lagging strand (forward reaction) (Figure 5A, lanes 7–9), as did a *bona fide* DnaB-like 5′→3′ hexameric DNA helicase (SPP1 G40P) (Figure 5A, lanes 3–4) (40,63). Similar results were observed when *wt* RadA/Sms was replaced by RadA/Sms C13A (Figure 5C, lanes 5–7) or RadA/Sms C13R (Supplementary Figure S5A, lanes 5–7), suggesting that the enzyme bound to the 5′-tail of the 3′-fork substrate unwinds DNA in the 5′→3′ direction.

Increasing RadA/Sms, RadA/Sms C13A or RadA/Sms C13R concentrations bound to the 3′-tail of the 5′-fork DNA failed to unzip this DNA substrate (Figure 5B, lanes 5–9, D and Supplementary Figure S5B, lanes 3–7). Similar results were observed when RadA/Sms was replaced by SPP1 G40P DNA helicase, because this enzyme has a strict 5′→3′ polarity (Figure 5B, lanes 3–4) (40,63).

RecA activates RadA/Sms to unwind a 5′-fork DNA substrate

To test whether RadA/Sms, upon interacting with RecA at a fork DNA, unwinds a cognate and non-cognate substrate, we examined the unwinding of a 3′- and 5′-fork DNA in the presence of RecA. RadA/Sms, bound to the 5′-tail, unwound the 3′-fork DNA in the 5′→3′ direction in the presence of increasing RecA concentrations. As described for a 5′-tailed substrate (Supplementary Figure S4A, C and E, lanes 14–15), at a 0.8:1 or higher RecA:RadA/Sms ratio, the efficiency of DNA unwinding was slightly reduced (Figure 5A, lanes 13 versus 15–17). Similar results were observed when RadA/Sms was replaced by RadA/Sms C13A (Figure 5C, lanes 11 versus 13–15) or RadA/Sms C13R (Supplementary Figure S5A, lanes 11 versus 13–15), suggesting that RecA competes with the loading of *wt* RadA/Sms or its mutant variants at the ssDNA-dsDNA junction.

In the presence of increasing RecA concentrations, a fixed RadA/Sms amount was sufficient to unzip the non-cognate 5′-fork DNA substrate (Figure 5B, lanes 16–19). When RadA/Sms was replaced by RadA/Sms C13A or C13R, however, the mutant variants failed to unwind the 5′-fork DNA substrate (Figure 5B and Supplementary Figure S5B, lanes 12–16), suggesting that the interaction among RecA and RadA/Sms is necessary to promote RadA/Sms unwinding of an apparent non-cognate substrate.

At pH 7.5 the RecA protein preferentially bind ssDNA rather than dsDNA (30–32). Four different alternatives were considered to explain how RadA/Sms unwinds the 5′-fork DNA substrate and the origin of the new observed DNA band in the presence of RecA at pH 7.5. In the first two conditions, RecA nucleates and polymerises on the 3′-tail of the forked substrate in the 5′→3′ direction, and away from the ssDNA-dsDNA junction (Supplementary Figure S6, red arrow); with the 5′-end of the RecA filament, at the fork junction, facilitating the spontaneous thermal fraying of DNA (Supplementary Figure S6i–ii) (31,32). In the first option, the 5′-end of the RecA filament interacts with and loads RadA/Sms on the parental lagging strand, to render a 3′-tailed duplex. Then, RecA loads RadA/Sms on the nascent lagging strand template and unwinds the lagging strand template (forward reaction) in the 5′→3′ direction (Supplementary Figure S4B, lanes 13–15 and Supplementary Figure S6i). Second, the 5′-end of the RecA filament at the ssDNA–dsDNA junction interacts with and loads RadA/Sms on the nascent lagging strand, which is unwound, leading to the accumulation of an unreplicated forked intermediate. Then, RadA/Sms assembles to the 5′-tail of the fork displaces RecA and unwinds template strands (forward reaction) (Supplementary Figure S6ii). Third, the 3′-end of the RecA filament might interact and load RadA/Sms at the parental leading strand with RadA/Sms promoting unwinding backwards in the 3′→5′ direction, leading first to a 3′-tailed duplex and then RecA loads RadA/Sms on the nascent lagging strand (forward reaction) (Supplementary Figure S6iii). Finally, the 5′-end of the RecA nucleoprotein filament might interact with and load RadA/Sms at the fork junction on the parental leading strand, and unwinding in a 3′→5′ direction (backward reaction) renders a 3′-tailed duplex substrate. Then, RecA filamented at the 3′-tail loads RadA/Sms on the nascent lagging strand, which is unwound (forward reaction) (Supplementary Figure S6iv).

To test whether RecA could promote RadA/Sms unwinding in the forward or backward direction, DNA intermediates were run in parallel to the previous helicase assay. As it can be seen, RadA/Sms unzipped the 5′-fork DNA substrate (Figure 5B, lanes 16–19), leading to the accumulation of an unreplicated fork intermediate, and in a second step unwound the fork to free the radiolabelled strand as depicted in Supplementary Figure S6ii. This result suggests that RadA polarity is not changed by the presence of RecA, but results in an unexpected activity, the unwinding of the nascent lagging strand, which mimics an invading 3′-end in a D-loop structure, that might be anti-recombinogenic during chromosomal transformation. Alternatively, RecA assembled on the 3′-end of the 5′-fork DNA substrate might branch migrate it, and expose the 5′-end of the nascent
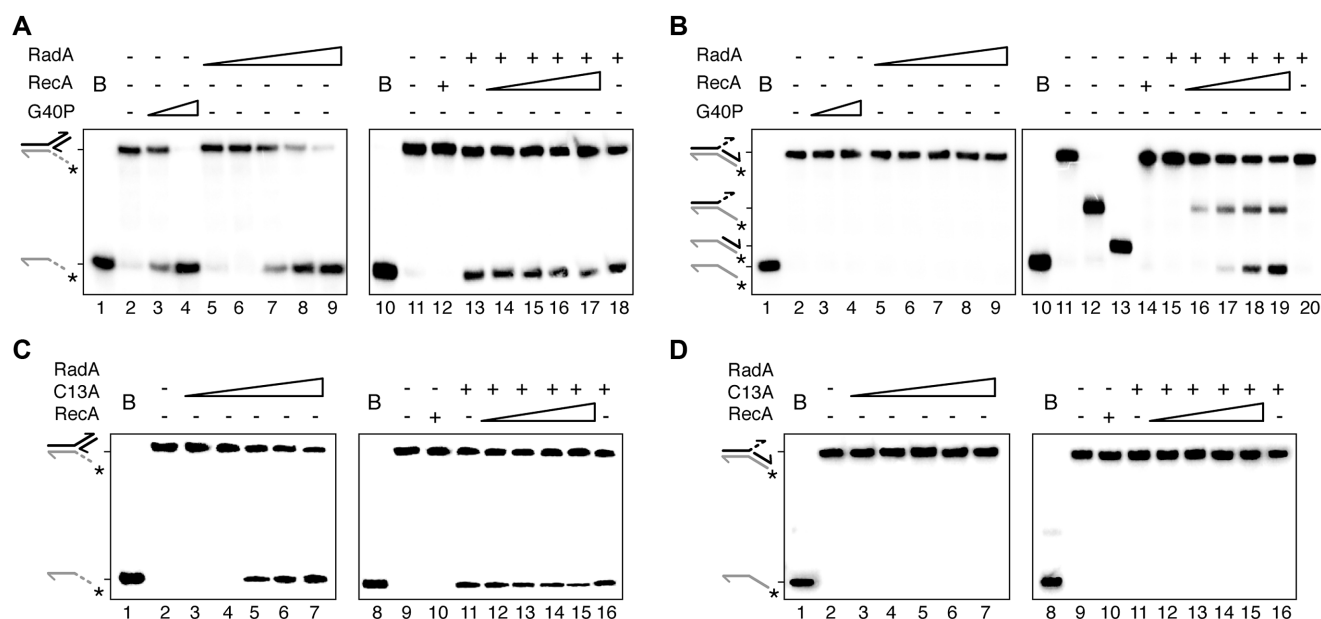
Figure 5. RecA loads RadA/Sms to unwind forked DNA in the 5′→3′ direction. Helicase assays with 3′-fork (**A** and **C**) and 5′-fork DNA (**B** and **D**) were performed with increasing concentrations of *wt* RadA/Sms (**A** and **B**) or RadA/Sms C13A (**C** and **D**) (30–500 nM) (denoted as RadA and RadA C13A) or a fixed concentration of *wt* RadA/Sms or RadA/Sms C13A (125 nM) and increasing RecA concentrations (50–400 nM). Reactions were done in buffer A containing 2 mM ATP (15 min, 30°C), and after deproteinization the substrate and products were separated by 10% PAGE and visualized by phosphor imaging. In parallel, the unwinding activity of the G40P replicative helicase (15 and 30 nM), which only unwinds 3′-fork DNA, was assayed. Abbreviations: B, boiled DNA substrate; - and +, absence and presence of the indicated protein; *, denotes the labelled 5′-end; half arrow head, denotes the 3′-end.

lagging strand to which RadA/Sms could bind and unwind the DNA substrate. Since RadA/Sms C13A or C13R cannot unwind this potentially RecA-mediated branch migrated substrates (Figure 5B and Supplementary Figure S5B, lanes 11–15) we have to assume an active role of RecA on RadA/Sms loading rather than a branch migration of the substrates.

RecA down regulates RadA/Sms unwinding of a 3′-invading D-loop

To test at which position(s) RadA/Sms is loaded, a 3′-invading D-loop DNA substrate was constructed and RadA/Sms-mediated DNA unwinding was next assayed (see Supplementary Figure S7). The 3′-invading D-loop DNA substrate (30-nt long 5′-tail region and 30-nt long displaced loop) was incubated with increasing *wt* RadA/Sms, RadA/Sms C13A or RadA/Sms C13R concentrations (15 min at 37°C), and DNA unwinding was measured. RadA/Sms or RadA/Sms C13A bound to the 5′-tail region of the radiolabelled invading strand unwound it with similar efficiency in the 5′→3′ direction (Supplementary Figure S7A, B, lanes 5–7). Similar results were observed when RadA/Sms C13A was replaced by RadA/Sms C13R (data not shown).

As with the 3′ fork DNA, the efficiency of RadA/Sms or RadA/Sms C13A unwinding of the 3′-invading D-loop DNA substrate decreased with increasing RecA concentrations (Supplementary Figure S7A, B, lanes 11 versus 14–15). It is likely therefore, that independently of a RecA-RadA/Sms interaction, RecA competes with RadA/Sms for the interaction with the invading ssDNA.

To test whether RecA regulates RadA/Sms unwinding of the 3′-invading D-loop, and if RecA sterically competes with RadA/Sms for binding to this DNA substrate, the D-loop substrate was preincubated first with RadA/Sms (5 min at 37°C) and then increasing RecA concentrations and ATP were added. The efficiency of RadA/Sms-mediated DNA unwinding did not decrease with increasing RecA concentrations (Supplementary Figure S7A, lanes 20 versus 23–24). Similar results were observed when RadA/Sms C13A was used (Supplementary Figure S7B, lanes 12–15 and 21–23) confirming that RecA competes with RadA/Sms or its variants for binding to the 5′-tail of the 3′-invading D-loop. This data suggests that RadA/Sms binding to its cognate substrate (the 5′-tailed of a 3′-invading D-loop) is highly efficient and masks the contribution of RecA-directed recruitment in the conditions addressed in Figure 1. However, if RadA binds to the 5′-tail of the 3′-invading strand, it would displace the invading strand, and thus reverse the transformation reaction, preventing recombination.

Then, we have searched for alternative substrates to study the role of RadA/Sms protein. Inactivation of *radA* renders cells deficient in gap and DSB repair (Supplementary Material, *Annex 3*, Figure 2B, C) (18). Repair of stalled and collapsed proceed throught a single or a double HJ intermediate, respectively, that may be processed by the RadA/Sms translocase. To study whether RadA/Sms processes HJ intermediates, a synthetic HJ DNA was radiolabelled and assayed. RadA/Sms bound HJ DNA (Supplementary Figure S2), but it failed to unzip this DNA substrate (Supplementary *Annex 5*, Supplementary Figure S8), thus the fate of

RadA/Sms on a synthetic 5′-invading D-loop DNA substrate was studied.

RecA promotes RadA/Sms unwinding of a 5′-invading D-loop

A 5′-invading D-loop DNA substrate was constructed and RadA/Sms-mediated DNA unwinding was next assayed (see Figure 6A). Increasing concentrations of *wt* RadA/Sms poorly unwound the 5′-invading radiolabelled strand to render a 3′-tailed duplex and a higher amount of the displaced invading strand (Figure 6B, lanes 6–7), but RadA/Sms C13A failed to unwind this 5′-invading D-loop substrate (Figure 6C, lanes 3–7).

We then analysed the unwinding activity of RadA/Sms on this substrate in the presence of RecA. Three different alternatives were considered depending on where RadA/Sms is loaded by RecA on this DNA substrate, which result in different unwinding intermediates. First, the 5′-end of the RecA filament bound to the displaced strand interacts with and loads RadA/Sms at the complementary strand on the template substrate (Figure 6A, position *a*) and/or the 3′-end of the RecA filament interacts with and loads RadA/Sms at the displaced strand (Figure 6A, *b*). This loading will first render a 3′-tailed duplex as intermediate. Then, the 5′-end of the RecA filament assembled at the 3′-tail interacts with and loads RadA/Sms at the duplex junction onto the invading strand to unwind it (Figure 6A, *e*). Second, the RecA filament assembled at the invading strand interacts with and loads RadA/Sms on the complementary strand (Figure 6A, *c*). RadA/Sms loaded on the complementary strand unwinds the substrate in the 5′→3′ direction to displace the invading strand (Figure 6A). Finally, the 5′-end of the RecA nucleoprotein filament assembled on the displaced strand interacts with and loads RadA/Sms on the invading strand (Figure 6A, *f*). RecA-mediated loading of RadA/Sms at positions *c* or *f* (Figure 6A) will result in unwinding of the invading strand, being anti-recombinogenic during chromosomal transformation.

When the 5′-invading D-loop DNA was incubated only with RadA/Sms, the displacement of the invading strand was ∼4-fold more efficient than the formation of a 3′-tailed duplex (Figure 6B, lanes 6–7, 11 and 20). This result suggested that RadA/Sms can be bound at positions *c* or *f* (as depicted in Figure 6A) to yield the main observed products. The DNA substrate was then pre-incubated with increasing RecA concentrations and a fixed RadA/Sms or RadA/Sms C13A amount (15 min at 37°C), and DNA unwinding of the radiolabelled strand was measured by addition of ATP. In the presence of RecA, RadA/Sms efficiently unwound the D-loop substrate to render higher or stoichiometric amounts of the 3′-tailed duplex intermediate with respect to the final product (Figure 6B, lanes 14–15). It is likely that RecA promotes the loading of RadA/Sms on positions *a* and *b* to yield the 3′-tailed duplex intermediate, and then RecA loads RadA/Sms at position *e* to render the displaced invading strand as depicted in Figure 6A and documented in Figure 6B, lanes 13–15). When RadA/Sms was replaced by RadA/Sms C13A, increasing RecA concentrations did not stimulate DNA unwinding (Figure 6C, lanes 12–15).

To limit the amount of available ssDNA, the D-loop substrate was pre-incubated with stoichiometric concentrations of SsbA (1 SsbA tetramer/ 33-nt). RecA cannot displace SsbA from the ssDNA (8,9). To test whether RadA/Sms displaces SsbA from the substrate, and if RecA can interact with and load RadA/Sms to unwind the 5′-invading D-loop substrate, the displaced strand and the 3′-tail of the invading strand were coated with SsbA. In the presence of SsbA, increasing RecA concentrations facilitated RadA/Sms-mediated unwinding of the 3′-tailed duplex intermediate with respect to the final product (Figure 6B, lanes 23–24), suggesting that RadA/Sms displaces SsbA, and RecA filamented on the ssDNA regions loads RadA/Sms onto the displaced strand (Figure 1A*ii*, position *b*) and on the opposite strand (Figure 1Aii, *a*) as depicted in (Figure 6A, positions *a* and *b*, and then position *e*)

RadA/Sms does not facilitate integration of divergent DNA sequences

In previous sections we have documented that: (i) RadA/Sms interacts with and down regulates RecA ATP hydrolysis rate (Figure 4C); (ii) a RecA nucleoprotein filament interacts with and loads RadA/Sms onto an apparent non-cognate 5′-fork or 5′-invading D-loop substrate (Figures 5 and 6); and iii) RadA/Sms catalyses DNA unwinding to expand the D-loop structure. We can envision two different mechanisms of action of RadA/Sms during natural transformation. The first hypothesis is that RecA loads RadA/Sms onto the D-loop, RadA/Sms promotes D-loop expansion independently of RecA, and indirectly facilitates the spontaneous annealing of the invading ssDNA. Since spontaneous annealing is insensitive to DNA mismatches, RadA/Sms might contribute to override the interspecies recombination barrier. Alternatively, RecA loads RadA/Sms onto the D-loop, then RadA/Sms promotes D-loop expansion in concert with RecA that constantly searches for homology to provide a barrier to DNA sequence divergence.

As revealed in Supplementary *Annex 6*, the frequency of interspecies chromosomal transformation decreased log-linearly with increasing sequence divergence up to ∼10% in competent Δ*radA* cells, but beyond 10% sequence divergence the transformation frequency marginally varied and was similar to the spontaneous mutation rate (5–9 × 10⁻⁹) (Supplementary Figure S9A). By contrast, the chromosomal transformation frequency decreased in a log-linear relationship up to ∼15% sequence divergence in the *rec*⁺ control (Supplementary Figure S9A) (37,38).

When the frequency of chromosomal transformation with homologous *rpoB*482 DNA in Δ*radA* cells was normalized to 1 (filled squares [normalized Δ*radA*]), the frequency of transformants up to ∼10% sequence divergence was similar to the *rec*⁺ strain (Supplementary Figure S9A), suggesting that RadA/Sms does not contribute to overcome the DNA sequence divergence barrier, and RecA might act in concert with RadA/Sms to maintain the genetic isolation.

Nucleotide sequence analyses of the integrated DNA show that the mean integration length of the 2,997-bp *rpoB*482 DNA decreased with increasing sequence diver-

Figure 6. RadA/Sms unwinds D-loop DNA. (**A**) Different outcomes after DNA unwinding by RadA/Sms depending on where it is loaded by the RecA protein on the 5′-invading D-loop intermediate. Left draw, the RecA filament bound to the displaced strand might interact with and load RadA/Sms at the complementary strand (position *a*) and on the displaced strand (*b*) to render a 3′-tailed duplex intermediate. Then, the RecA filament assembled at the 3′-tailed duplex intermediate interacts with and loads RadA/Sms at the duplex junction into a generated 5′-flap to unwind the 3′-tailed duplex (*e*). Central draw, the RecA filament assembled on the invading strand might interact with and load RadA/Sms on the complementary strand (*c*). Then, RadA/Sms unwinds the substrate in the 5′→3′ direction to reverse the invading reaction. Right draw, the 5′-end of the RecA nucleoprotein filament assembled on the displaced strand interacts with and loads RadA/Sms on the invading DNA (*f*), to displace the invading strand. (**B**) Increasing RadA/Sms concentrations (30 to 500 nM, lanes 3–7) were incubated with the 5′-invading D-loop in buffer A containing 2 mM ATP (15 min, 30°C). A fix RadA/Sms (125 nM, lanes 11–16) concentration was incubated with increasing RecA concentrations (50 to 400 nM, lanes 12–15) and with the 5′-invading D-loop (15 min, 30°C) and the substrate and products were separated. The 5′-invading D-loop substrate was pre-incubated with SsbA (300 nM, lanes 21–24) (5 min, 30°C), then RadA/Sms and increasing RecA concentrations were added, the reaction incubated in buffer A containing 2 mM ATP (15 min, 30°C), and stopped by deproteinization. (**C**) Increasing concentrations of RadA/Sms C13A (30–500 nM, lanes 2–7) (denoted as RadA C13A) or a fixed concentration of RadA/Sms C13A (125 nM) and increasing RecA concentrations (50–400 nM, lanes 12–15) were incubated in buffer A containing 2 mM ATP (15 min, 30°C). After deproteinization, the substrate and products were separated by 10% PAGE and visualized by phosphor imaging. Abbreviations as those in Figure 5.

gence up to 10.2% sequence divergence, whereas in the *rec*[+] control genuine transformants are detected up to 14.5% sequence divergence (Supplementary *Annex 6*, Supplementary Figure S9B). At 10.2% sequence divergence, the Rif[R] recombinants had a moderate increase in the integration length in the Δ*radA* strain when compared with the *rec*[+] control (Supplementary Figure S9B). It is likely that RadA/Sms helps RecA to promote interspecies chromosomal transformation with ∼15% sequence divergence, and RadA/Sms has to work in concert with RecA to maintain the speciation of the species.

DISCUSSION

This study aims to decipher the molecular mechanism of *B. subtilis* RadA/Sms in natural transformation. RadA/Sms is necessary for HR between fully homologous DNAs (repair-by-recombination and genetic recombination by chromosomal transformation), and to increase the rate of interspecies chromosomal transformation between partially homologous sequences. We show that absence of RadA/Sms decreases by ∼140-fold chromosomal transformation, and the remaining recombination proficiency in Δ*radA* cells can be attributed to the RecG translocase. Lack of both

RadA/Sms and RecG blocked chromosomal transformation, and reduced plasmid transformation ∼200-fold when compared to *rec*^{+} cells (Figure 2A), suggesting that both RadA/Sms and RecG contribute to the destabilization of the RecA nucleoprotein filaments. These results also suggest that there is a division of labour, RadA/Sms is the major branch migrating translocase of D-loop intermediates, as during natural chromosomal transformation, but it cannot unwind HJ structures (Supplementary *Annex 5*, Supplementary Figure S8). On the other hand, RecG is the main branch migrating translocase of isomers of D-loops (a stalled replication fork) towards HJ structures during DNA damage tolerance and canonical DSB repair (54,55).

RadA/Sms mutations in the C4 motif poisoned both chromosomal and plasmid transformation, but the absence of RecA suppressed the plasmid transformation defect. Two non-mutually exclusive RadA/Sms activities might reasonably explain these phenotypes. In the first activity, which is crucial for chromosomal transformation, a RecA filament invades a homologous region with a dynamic assembly/disassembly from the incoming ssDNA and on the displaced strand at the formed D-loop intermediates (Figure 1A). RadA/Sms interacts with RecA and inhibits its ATPase activity, to decrease the dynamic disassembly. A more static RecA interacts with and loads RadA/Sms at positions *a* and *b* (Figure 1Aii–iii). Then, RadA/Sms branch migrates and extends the D-loop to facilitate the acquisition of the incoming homologous linear ssDNA, in concert with RecA, with a division of labour between both proteins. One (or two) RadA/Sms hexamer(s) catalyses (divergently) heteroduplex expansion of the D-loop structure, and in concert with RecA, provide a barrier to the acquisition of DNA with up to 15% sequence divergence in the *rec*[+] control. Indeed, RecA in its continuous search for homology warrants the '*self*' rather than the assimilation of '*non-self*' DNA. In contrast, RadA of γ-Proteobacteria is not the translocase that extends the D-loop intermediate during chromosomal transformation (22) or during Hfr chromosomal conjugation (23,24). It is likely that in the distantly related Firmicutes and Proteobacteria Phyla a different branch migration translocase extends the D-loop intermediate during natural chromosomal transformation and Hfr conjugation. In the second activity, which plays a crucial role in natural plasmid transformation, RecA assembled on the heterologous plasmid DNA, upon interacting with *wt* RadA/Sms, is prone to dissociation by a genuine negative RecA modulator (recX, RecU) (58,59,64). Indeed, RadA/Sms interacts with and reduces the ATPase activity of RecA and might indirectly facilitate RecA dissociation from the ssDNA.

In vitro, the RadA/Sms C13A or C13R mutant in the apo form preferentially binds ssDNA (Supplementary Figure S2). Similar results were observed when RadA*Spn* C27A was analysed (20). In contrast, the RadA*Eco* C28Y mutant was defective in DNA binding, and *wt* RadA*Eco* only binds poly(dT) DNA in the presence of ADP (21). RadA/Sms C13A or C13R, upon binding to cssDNA, show a stimulation of their ATPase activity (Figure 4), whereas the ATPase activity of *wt* RadA/Sms was insensitive to the presence of cssDNA. Since RecA physically interacts with RadA/Sms (Supplementary material *Annex 4*) it was hypothesized that RecA might load RadA/Sms onto cssDNA

and activate its ssDNA-dependent ATPase activity. RecA bound to cssDNA does not stimulate the ATPase activity of RadA/Sms; the opposite was observed. Independently of the order of addition, the presence of RadA/Sms seems to downregulate the maximal rate of RecA-mediated ATP hydrolysis. To test whether the ATPase activity of RecA was inhibited, RadA/Sms was replaced by the catalytically inactive Walker A RadA/Sms K104R mutant that does not bind ATP. In the presence of RadA/Sms K104R, the ATPase activity of RecA is restrained, indicating that RadA/Sms·ATP, upon interacting with RecA might reduce its dynamics and filament growth, but RadA/Sms might maintain its own ATPase activity because it can unwind an apparent non-cognate substrates in the presence of RecA. This effect was attributed to a direct RecA-RadA/Sms interaction, because when RadA/Sms was replaced by RadA/Sms C13A or RadA/Sms C13R, which fails to interact with RecA, the maximal rate of ATP hydrolysis of both proteins was not affected. RadA/Sms might act as a cap at the 5′-end of the RecA filament to down regulate RecA-mediated ATP hydrolysis and indirectly reduce the dynamics of RecA nucleoprotein filament formation. This effect might facilitate loading of a hexameric RadA/Sms ring at the ssDNA–dsDNA junction. Stoichiometric SsbA concentrations slightly reduce the ATPase of RadA/Sms C13A and the helicase activity of RadA/Sms or RadA/Sms C13A, but RecA cannot nucleate onto SsbA–ssDNA complexes (8). Here, we show that: (i) RadA/Sms might displace SsbA from the ssDNA and load RecA onto SsbA-coated ssDNA and (ii) RecA, loaded in the absence of mediators, facilitates RadA/Sms-mediated unwinding of apparent noncognate substrates by working as a ring-breaker to load the RadA/Sms hexameric ring to migrate a D-loop structure in the 5′→3′ direction.

Unlike RadA*Eco* that lacks a DNA helicase activity but stimulates the branch migration phase of RecA*Eco*-mediated strand transfer reactions (21), RadA/Sms, RadA*Spn* and their mutant variants in the C4 motif bind to the 5′-tail of a duplex or of a 3′-fork substrates and unwind them in the 5′→3′ direction (Supplementary Figure S4A and Figure 5A and C) (18,20). The presence of RecA, which polymerises on the 5′-tail towards the ssDNA-dsDNA junction, partially compete with RadA/Sms or RadA/Sms variants for ssDNA binding and DNA unwinding.

RadA/Sms cannot unwind the non-cognate (3′-tail duplex or 5′-fork) substrate. RecA interacts with and loads *wt* RadA/Sms, that unwinds the substrate in the 5′→3′ direction. It is likely that RecA filamented on the incoming ssDNA upon encountering a homologous sequence, promotes D-loop formation. Then, RecA bound to the invading or to the displaced strand facilitates the loading of the RadA/Sms hexameric ring-shaped helicase to produce long heteroduplex regions. RadA/Sms separates genomic duplex DNA strands in the 5′→3′ direction and helps RecA to integrate the incoming ssDNA. How this occurs mechanistically remains to be determined. The 5′-end of the RecA filament, assembled in the 3′-tail of a 5′-fork substrate, interacts with and loads *wt* RadA/Sms at the opposite strand on the 5′-flap of the nascent lagging strand to separate the paired strands in the 5′→3′ direction (anti-recombinase activity) (Figure 5B, lanes 16–19, as depicted in Supplementary Fig-

ure S6ii). When a 5′-invading D-loop intermediate was analysed, however, two major and a minor loading steps were documented. The 5′-end of the RecA filament, formed on the displaced strand, interacts with and loads RadA/Sms at the complementary strand (Figure 6A, position *a* and Figure 1Aii-iii, position *a*), and the 3′-end of the RecA filament interacts with and loads RadA/Sms on the same strand (Figure 1Aii–iii, position *b*). RecA recruits RadA/Sms on each strand of the recipient dsDNA, at positions *a* and *b*, and they migrate divergently to facilitate incorporation of invading ssDNA in the D-loop substrate. In our assay, a 3′-tailed substrate is accumulated. Thus, the 5′-end of the RecA filament interacts with and loads RadA/Sms at the 5′-end of the invading strand with low efficiency (Figure 6A, position *f*) or the frayed on the nascent lagging (Figure 3B, lanes 16–19 as depicted in Supplementary Figure S6*ii*). It is likely that another unknown activity, missing in our reaction, must down regulate this anti-recombinase activity during chromosomal transformation and direct RadA/Sms towards positions *a* and *b* (see Figure 1Aii–iii, position *a* and *b*).

RadA/Sms is also required for repair-by-recombination (Figure 2B, C). During two-ended DSB repair, cleaved DNA ends are resected, by different end-processing 5′ →3′ exonucleases, to produce 3′-ended ssDNA tails, which are initially coated by SsbA (7,12,65). The two-component RecA mediator (SsbA and RecO [RecO-RecR *in vivo*]) facilitates RecA nucleation and filament growth on the SsbA-ssDNA-RecO complex to render an active RecA nucleoprotein filament (9). RecA assembled in the 3′-tailed duplex DNA engages in a genome-wide search for a homologous segment on the intact sister chromosome. Once the homologous sequence in encountered, RecA catalyses strand invasion to form a plectonemic D-loop and to nucleate in the displaced strand, the initial steps in repair (Figure 1B). If our working model is correct, the 5′-end of the RecA filament, assembled on the displaced strand, loads RadA/Sms on the opposite strand (Figure 1B, position *a*) and the 3′-end of the RecA filament loads RadA/Sms on the same strand (Figure 1B, position *b*). RadA/Sms loaded at position *b* might expand the D-loop to favour DNA synthesis to restore genetic material lost by resection, and second end capture with subsequent DNA synthesis to restore genetic material lost by resection (Figure 1Bii–iii, positions *b*). These could be a common step for canonical DSB and SDSA repair. For SDSA repair, we predict that RadA/Sms loading at positions *a* and *b* may be turned off by a poorly characterized function and RecA might load RadA/Sms at positions *c* and *d* to favour the disruption of the D-loop (strand pullout) (Figure 1Biv-v). The complementary displaced DNA ends might be annealed by a process termed SDSA, facilitating the recovery of non-crossover DSBs. This is consistent with the fact that: i) RadA/Sms translocates D-loop structures (Figure 6) (20) rather than HJ intermediates (Supplementary Figure S8); and ii) RadA$_{Dra}$, in concert with RecA$_{Dra}$, contributes to extended SDSA (35). It is likely that a trade-off between RecA-directed loading at positions *a* and *b* (Figure 1Aii–iii) for chromosomal transformation and loading at positions *c* and *d* (Figure 1Biv-v) for SDSA repair exists. It will be of significant interest to

understand the factor(s) that regulate the selective recruitment of RadA/Sms during chromosomal transformation and SDSA repair. More investigation is needed to clarify the details of the model.

SUPPLEMENTARY DATA

Supplementary Data are available at NAR Online.

REFERENCES

1. Gogarten,J.P., Doolittle,W.F. and Lawrence,J.G. (2002) Prokaryotic evolution in light of gene transfer. *Mol. Biol. Evol.*, **19**, 2226–2238.
2. Fraser,C., Hanage,W.P. and Spratt,B.G. (2007) Recombination and the nature of bacterial speciation. *Science*, **315**, 476–480.
3. Chen,I. and Dubnau,D. (2004) DNA uptake during bacterial transformation. *Nat. Rev. Microbiol.*, **2**, 241–249.
4. Claverys,J.P., Martin,B. and Polard,P. (2009) The genetic transformation machinery: composition, localization, and mechanism. *FEMS Microbiol. Rev.*, **33**, 643–656.
5. Kidane,D., Ayora,S., Sweasy,J.B., Graumann,P.L. and Alonso,J.C. (2012) The cell pole: the site of cross talk between the DNA uptake and genetic recombination machinery. *Crit. Rev. Biochem. Mol. Biol.*, **47**, 531–555.
6. Yadav,T., Carrasco,B., Hejna,J., Suzuki,Y., Takeyasu,K. and Alonso,J.C. (2013) *Bacillus subtilis* DprA Recruits RecA onto Single-stranded DNA and Mediates Annealing of Complementary Strands Coated by SsbB and SsbA. *J. Biol. Chem.*, **288**, 22437–22450.
7. Yadav,T., Carrasco,B., Myers,A.R., George,N.P., Keck,J.L. and Alonso,J.C. (2012) Genetic recombination in *Bacillus subtilis*: a division of labor between two single-strand DNA-binding proteins. *Nucleic Acids Res.*, **40**, 5546–5559.
8. Yadav,T., Carrasco,B., Serrano,E. and Alonso,J.C. (2014) Roles of *Bacillus subtilis* DprA and SsbA in RecA-mediated genetic recombination. *J. Biol. Chem.*, **289**, 27640–27652.
9. Carrasco,B., Yadav,T., Serrano,E. and Alonso,J.C. (2015) *Bacillus subtilis* RecO and SsbA are crucial for RecA-mediated recombinational DNA repair. *Nucleic. Acids. Res.*, **43**, 5984–5997.
10. Lovett,C.M. Jr. and Roberts,J.W. (1985) Purification of a RecA protein analogue from *Bacillus subtilis*. *J. Biol. Chem.*, **260**, 3305–3313.
11. Steffen,S.E., Katz,F.S. and Bryant,F.R. (2002) Complete inhibition of *Streptococcus pneumoniae* RecA protein-catalyzed ATP hydrolysis by single-stranded DNA-binding protein (SSB protein): implications for the mechanism of SSB protein-stimulated DNA strand exchange. *J. Biol. Chem.*, **277**, 14493–14500.
12. Manfredi,C., Carrasco,B., Ayora,S. and Alonso,J.C. (2008) *Bacillus subtilis* RecO nucleates RecA onto SsbA-coated single-stranded DNA. *J. Biol. Chem.*, **283**, 24837–24847.
13. Carrasco,B., Manfredi,C., Ayora,S. and Alonso,J.C. (2008) *Bacillus subtilis* SsbA and dATP regulate RecA nucleation onto single-stranded DNA. *DNA Repair (Amst.)*, **7**, 990–996.

14. Kidane,D. and Graumann,P.L. (2005) Intracellular protein and DNA dynamics in competent *Bacillus subtilis* cells. *Cell*, **122**, 73–84.

15. Kidane,D., Carrasco,B., Manfredi,C., Rothmaier,K., Ayora,S., Tadesse,S., Alonso,J.C. and Graumann,P.L. (2009) Evidence for different pathways during horizontal gene transfer in competent *Bacillus subtilis* cells. *PLoS Genet.*, **5**, e1000630.

16. Song,Y. and Sargentini,N.J. (1996) *Escherichia coli* DNA repair genes *radA* and *sms* are the same gene. *J. Bacteriol.*, **178**, 5045–5048.

17. Cañas,C., Suzuki,Y., Marchisone,C., Carrasco,B., Freire-Beneitez,V., Takeyasu,K., Alonso,J.C. and Ayora,S. (2014) Interaction of branch migration translocases with the Holliday junction-resolving enzyme and their implications in Holliday junction resolution. *J. Biol. Chem.*, **289**, 17634–17646.

18. Torres,R., Serrano,E., Tramm,K. and Alonso,J.C. (2019) *Bacillus subtilis* RadA/Sms contributes to chromosomal transformation and DNA repair in concert with RecA and circumvents replicative stress in concert with DisA. *DNA Repair (Amst.)*, **77**, 45–57.

19. Burghout,P., Bootsma,H.J., Kloosterman,T.G., Bijlsma,J.J., de Jongh,C.E., Kuipers,O.P. and Hermans,P.W. (2007) Search for genes essential for pneumococcal transformation: the RadA DNA repair protein plays a role in genomic recombination of donor DNA. *J. Bacteriol.*, **189**, 6540–6550.

20. Marie,L., Rapisarda,C., Morales,V., Berge,M., Perry,T., Soulet,A.L., Gruget,C., Remaut,H., Fronzes,R. and Polard,P. (2017) Bacterial RadA is a DnaB-type helicase interacting with RecA to promote bidirectional D-loop extension. *Nat. Commun.*, **8**, 15638.

21. Cooper,D.L. and Lovett,S.T. (2016) Recombinational branch migration by the RadA/Sms paralog of RecA in Escherichia coli. *Elife*, **5**, e10807.

22. Nero,T.M., Dalia,T.N., Wang,J.C., Kysela,D.T., Bochman,M.L. and Dalia,A.B. (2018) ComM is a hexameric helicase that promotes branch migration during natural transformation in diverse Gram-negative species. *Nucleic Acids Res.*, **46**, 6099–6111.

23. Beam,C.E., Saveson,C.J. and Lovett,S.T. (2002) Role for *radA/sms* in recombination intermediate processing in *Escherichia coli*. *J. Bacteriol.*, **184**, 6836–6844.

24. Cooper,D.L., Boyle,D.C. and Lovett,S.T. (2015) Genetic analysis of *Escherichia coli* RadA: functional motifs and genetic interactions. *Mol. Microbiol.*, **95**, 769–779.

25. Carrasco,B., Fernandez,S., Asai,K., Ogasawara,N. and Alonso,J.C. (2002) Effect of the *recU* suppressors *sms* and *subA* on DNA repair and homologous recombination in *Bacillus subtilis*. *Mol. Genet. Genomics*, **266**, 899–906.

26. Gándara,C., de Lucena,D.K.C., Torres,R., Serrano,E., Altenburger,S., Graumann,P.L. and Alonso,J.C. (2017) Activity and in vivo dynamics of *Bacillus subtilis* DisA are affected by RadA/Sms and by Holliday junction-processing proteins. *DNA Repair (Amst.)*, **55**, 17–30.

27. Inoue,M., Fukui,K., Fujii,Y., Nakagawa,N., Yano,T., Kuramitsu,S. and Masui,R. (2017) The Lon protease-like domain in the bacterial RecA paralog RadA is required for DNA binding and repair. *J. Biol. Chem.*, **292**, 9801–9814.

28. Itsathitphaisarn,O., Wing,R.A., Eliason,W.K., Wang,J. and Steitz,T.A. (2012) The hexameric helicase DnaB adopts a nonplanar conformation during translocation. *Cell*, **151**, 267–277.

29. Singleton,M.R., Dillingham,M.S. and Wigley,D.B. (2007) Structure and mechanism of helicases and nucleic acid translocases. *Annu. Rev. Biochem.*, **76**, 23–50.

30. Radding,C.M. (1991) Helical interactions in homologous pairing and strand exchange driven by RecA protein. *J. Biol. Chem.*, **266**, 5355–5358.

31. Cox,M.M. (2007) Motoring along with the bacterial RecA protein. *Nat. Rev. Mol. Cell Biol.*, **8**, 127–138.

32. Bell,J.C. and Kowalczykowski,S.C. (2016) RecA: Regulation and Mechanism of a Molecular Search Engine. *Trends Biochem. Sci.*, **41**, 491–507.

33. Dubnau,D. and Cirigliano,C. (1972) Fate of transforming deoxyribonucleic acid after uptake by competent *Bacillus subtilis*: size and distribution of the integrated donor segments. *J. Bacteriol.*, **111**, 488–494.

34. Fornili,S.L. and Fox,M.S. (1977) Electron microscope visualization of the products of *Bacillus subtilis* transformation. *J. Mol. Biol.*, **113**, 181–191.

35. Slade,D., Lindner,A.B., Paul,G. and Radman,M. (2009) Recombination and replication in DNA repair of heavily irradiated *Deinococcus radiodurans*. *Cell*, **136**, 1044–1055.

36. Gassel,M. and Alonso,J.C. (1989) Expression of the *recE* gene during induction of the SOS response in *Bacillus subtilis* recombination-deficient strains. *Mol. Microbiol.*, **3**, 1269–1276.

37. Carrasco,B., Serrano,E., Sanchez,H., Wyman,C. and Alonso,J.C. (2016) Chromosomal transformation in *Bacillus subtilis* is a non-polar recombination reaction. *Nucleic. Acids. Res.*, **44**, 2754–2768.

38. Carrasco,B., Serrano,E., Martin-Gonzalez,A., Moreno-Herrero,F. and Alonso,J.C. (2019) *Bacillus subtilis* MutS modulates RecA-mediated DNA strand exchange between divergent DNA sequences. *Front. Microbiol.*, **10**, 237.

39. Maciag,I.E., Viret,J.F. and Alonso,J.C. (1988) Replication and incompatibility properties of plasmid pUB110 in *Bacillus subtilis*. *Mol. Gen. Genet.*, **212**, 232–240.

40. Ayora,S., Weise,F., Mesa,P., Stasiak,A. and Alonso,J.C. (2002) *Bacillus subtilis* bacteriophage SPP1 hexameric DNA helicase, G40P, interacts with forked DNA. *Nucleic Acids Res.*, **30**, 2280–2289.

41. Battesti,A. and Bouveret,E. (2012) The bacterial two-hybrid system based on adenylate cyclase reconstitution in *Escherichia coli*. *Methods*, **58**, 325–334.

42. Alonso,J.C., Tailor,R.H. and Luder,G. (1988) Characterization of recombination-deficient mutants of *Bacillus subtilis*. *J. Bacteriol.*, **170**, 3001–3007.

43. Ceglowski,P., Luder,G. and Alonso,J.C. (1990) Genetic analysis of *recE* activities in *Bacillus subtilis*. *Mol. Gen. Genet.*, **222**, 441–445.

44. Sanchez,H., Carrasco,B., Cozar,M.C. and Alonso,J.C. (2007) *Bacillus subtilis* RecG branch migration translocase is required for DNA repair and chromosomal segregation. *Mol. Microbiol.*, **65**, 920–935.

45. Carrasco,B., Ayora,S., Lurz,R. and Alonso,J.C. (2005) *Bacillus subtilis* RecU Holliday-junction resolvase modulates RecA activities. *Nucleic. Acids. Res.*, **33**, 3942–3952.

46. Shereda,R.D., Kozlov,A.G., Lohman,T.M., Cox,M.M. and Keck,J.L. (2008) SSB as an organizer/mobilizer of genome maintenance complexes. *Crit. Rev. Biochem. Mol. Biol.*, **43**, 289–318.

47. Chen,Z., Yang,H. and Pavletich,N.P. (2008) Mechanism of homologous recombination from the RecA-ssDNA/dsDNA structures. *Nature*, **453**, 489–484.

48. Ayora,S., Carrasco,B., Doncel-Perez,E., Lurz,R. and Alonso,J.C. (2004) *Bacillus subtilis* RecU protein cleaves Holliday junctions and anneals single-stranded DNA. *Proc. Natl. Acad. Sci. U.S.A.*, **101**, 452–457.

49. McGregor,N., Ayora,S., Sedelnikova,S., Carrasco,B., Alonso,J.C., Thaw,P. and Rafferty,J. (2005) The structure of *Bacillus subtilis* RecU Holliday junction resolvase and its role in substrate selection and sequence-specific cleavage. *Structure*, **13**, 1341–1351.

50. Zecchi,L., Lo Piano,A., Suzuki,Y., Canas,C., Takeyasu,K. and Ayora,S. (2012) Characterization of the Holliday junction resolving enzyme encoded by the *Bacillus subtilis* bacteriophage SPP1. *PLoS ONE*, **7**, e48440.

51. Torres,R., Carrasco,B., Gandara,C., Baidya,A.K., Ben-Yehuda,S. and Alonso,J.C. (2019) *Bacillus subtilis* DisA regulates RecA-mediated DNA strand exchange. *Nucleic Acids Res.*, **47**, 5141–5154.

52. Sanchez,H., Kidane,D., Reed,P., Curtis,F.A., Cozar,M.C., Graumann,P.L., Sharples,G.J. and Alonso,J.C. (2005) The RuvAB branch migration translocase and RecU Holliday junction resolvase are required for double-stranded DNA break repair in *Bacillus subtilis*. *Genetics*, **171**, 873–883.

53. West,S.C. (2003) Molecular views of recombination proteins and their control. *Nat. Rev. Mol. Cell Biol.*, **4**, 435–445.

54. Atkinson,J. and McGlynn,P. (2009) Replication fork reversal and the maintenance of genome stability. *Nucleic. Acids. Res.*, **37**, 3475–3492.

55. Gupta,S., Yeeles,J.T. and Marians,K.J. (2014) Regression of replication forks stalled by leading-strand template damage: I. both RecG and RuvAB catalyze regression, but RuvC cleaves the Holliday junctions formed by RecG preferentially. *J. Biol. Chem.*, **289**, 28376–28387.

56. Singleton,M.R., Scaife,S. and Wigley,D.B. (2001) Structural analysis of DNA replication fork reversal by RecG. *Cell*, **107**, 79–89.

57. Raguse,M., Torres,R., Seco,E.M., Gandara,C., Ayora,S., Moeller,R. and Alonso,J.C. (2017) *Bacillus subtilis* DisA helps to circumvent

replicative stress during spore revival. *DNA Repair (Amst.)*, **59**, 57–68.

58. Le,S., Serrano,E., Kawamura,R., Carrasco,B., Yan,J. and Alonso,J.C. (2017) *Bacillus subtilis* RecA with DprA-SsbA antagonizes RecX function during natural transformation. *Nucleic Acids Res.*, **45**, 8873–8885.

59. Serrano,E., Carrasco,B., Gilmore,J.L., Takeyasu,K. and Alonso,J.C. (2018) RecA Regulation by RecU and DprA During *Bacillus subtilis* Natural Plasmid Transformation. *Front Microbiol.*, **9**, 1514.

60. Kaplan,D.L. (2000) The 3′-tail of a forked-duplex sterically determines whether one or two DNA strands pass through the central channel of a replication-fork helicase. *J. Mol. Biol.*, **301**, 285–299.

61. Makowska-Grzyska,M. and Kaguni,J.M. (2010) Primase directs the release of DnaC from DnaB. *Mol. Cell*, **37**, 90–101.

62. Bailey,S., Eliason,W.K. and Steitz,T.A. (2007) Structure of hexameric DnaB helicase and its complex with a domain of DnaG primase. *Science*, **318**, 459–463.

63. Wang,G., Klein,M.G., Tokonzaba,E., Zhang,Y., Holden,L.G. and Chen,X.S. (2008) The structure of a DnaB-family replicative helicase and its interactions with primase. *Nat. Struct. Mol. Biol.*, **15**, 94–100.

64. Cardenas,P.P., Carrasco,B., Defeu Soufo,C., Cesar,C.E., Herr,K., Kaufenstein,M., Graumann,P.L. and Alonso,J.C. (2012) RecX facilitates homologous recombination by modulating RecA activities. *PLoS Genet.*, **8**, e1003126.

65. Ayora,S., Carrasco,B., Cardenas,P.P., Cesar,C.E., Canas,C., Yadav,T., Marchisone,C. and Alonso,J.C. (2011) Double-strand break repair in bacteria: a view from *Bacillus subtilis*. *FEMS Microbiol. Rev.*, **35**, 1055–1081.